

Award Number: W81XWH-04-1-0080

TITLE: Biomarkers of Selenium Action in Prostate Cancer

PRINCIPAL INVESTIGATOR: Jacques Lapointe

CONTRACTING ORGANIZATION: Stanford University
Stanford, CA 94305

REPORT DATE: March 2006

TYPE OF REPORT: Annual Summary

PREPARED FOR: U.S. Army Medical Research and Materiel Command
Fort Detrick, Maryland 21702-5012

DISTRIBUTION STATEMENT: Approved for Public Release;
Distribution Unlimited

The views, opinions and/or findings contained in this report are those of the author(s) and should not be construed as an official Department of the Army position, policy or decision unless so designated by other documentation.

REPORT DOCUMENTATION PAGE

Form Approved
OMB No. 0704-0188

Public reporting burden for this collection of information is estimated to average 1 hour per response, including the time for reviewing instructions, searching existing data sources, gathering and maintaining the data needed, and completing and reviewing this collection of information. Send comments regarding this burden estimate or any other aspect of this collection of information, including suggestions for reducing this burden to Department of Defense, Washington Headquarters Services, Directorate for Information Operations and Reports (0704-0188), 1215 Jefferson Davis Highway, Suite 1204, Arlington, VA 22202-4302. Respondents should be aware that notwithstanding any other provision of law, no person shall be subject to any penalty for failing to comply with a collection of information if it does not display a currently valid OMB control number. **PLEASE DO NOT RETURN YOUR FORM TO THE ABOVE ADDRESS.**

1. REPORT DATE 01-03-2006		2. REPORT TYPE Annual Summary		3. DATES COVERED 1 Jan 2004 – 28 Feb 2006	
4. TITLE AND SUBTITLE Biomarkers of Selenium Action in Prostate Cancer				5a. CONTRACT NUMBER	
				5b. GRANT NUMBER W81XWH-04-1-0080	
				5c. PROGRAM ELEMENT NUMBER	
6. AUTHOR(S) Jacques Lapointe				5d. PROJECT NUMBER	
				5e. TASK NUMBER	
				5f. WORK UNIT NUMBER	
7. PERFORMING ORGANIZATION NAME(S) AND ADDRESS(ES) Stanford University Stanford, CA 94305				8. PERFORMING ORGANIZATION REPORT NUMBER	
9. SPONSORING / MONITORING AGENCY NAME(S) AND ADDRESS(ES) U.S. Army Medical Research and Materiel Command Fort Detrick, Maryland 21702-5012					
10. SPONSOR/MONITOR'S ACRONYM(S)				11. SPONSOR/MONITOR'S REPORT NUMBER(S)	
13. SUPPLEMENTARY NOTES Original contains colored plates: ALL DTIC reproductions will be in black and white.					
14. ABSTRACT This study was designed to identify new, mechanistically relevant biomarkers of selenium responsiveness for use in intervention trials. We have characterized the global transcriptional response of LNCaP prostate cancer cells to selenium by using cDNA microarray. We have identified molecular targets of selenium that are secretory using bioinformatics approaches and datasets of selenium modulated transcripts and membrane bound and secretory proteins. To help prioritizing biomarker candidates, we have cross-referenced the selenium modulated genes list with existing prostate cancer microarray data sets. Using this approach, we have narrowed down the number of biomarker candidates that we are now characterizing in more details.					
15. SUBJECT TERMS Biomarkers, selenium, prostate cancer, microarray					
16. SECURITY CLASSIFICATION OF:				UU	18. NUMBER OF PAGES 42
a. REPORT U	b. ABSTRACT U	c. THIS PAGE U	19a. NAME OF RESPONSIBLE PERSON USAMRMC		
				19b. TELEPHONE NUMBER <i>(include area code)</i>	

Table of Contents

Cover	1
SF 298	2
Introduction	4
Body	4
Key Research Accomplishments	5
Reportable Outcomes	5
Conclusions	5
References	5
Appendices	6

Introduction Biomarkers of selenium actions in prostate tissue would be of great value in stratifying patients and monitoring the study subject compliance in clinical trials. We hypothesized that a subset of genes that show expression changes after selenium supplementation encode secretory proteins that can be detected in serum and serve as biomarkers of response to selenium. To identify such biomarkers, we proposed to identify molecular targets of selenium that are secretory using bioinformatics approaches and datasets of selenium modulated transcripts and membrane bound and secretory proteins.

Body Methylseleninic acid (MSA) has been shown to have potent anticancer activity and is an excellent compound for studying the anticancer effect of selenium in vitro. The global transcriptional response of LNCaP prostate cancer cell line to MSA was characterized using cDNA microarray¹. The expression of 1128 transcripts corresponding to 809 genes showed striking dose- and time-dependent changes in response to 3-30 μ M MSA over the time course of 48 h. Transcript levels of many cell cycle-regulated genes change in response to MSA, suggesting that MSA inhibits proliferation. Consistent with these gene expression changes, cell proliferation, monitored by carboxyfluorescein succinimidyl ester staining, was decreased after MSA treatment, and an accumulation of cells at G0/G1 phase was detected by flow cytometry. Surprisingly, MSA also modulated expression of many androgen-regulated genes, suppressed androgen receptor (AR) expression at both mRNA and protein level, and decreased levels of prostate specific antigen secreted into the medium. Low concentrations of MSA also induced significant increases in transcript levels of phase 2 detoxification enzymes and induced NADPH dehydrogenase, quinone 1 enzymatic activity, a surrogate marker of global phase 2 enzyme activity. Our results suggest that MSA may protect against prostate cancer by inhibiting cell proliferation, by modulating the expression of AR and AR-regulated genes and by inducing carcinogen defenses.

Since a large number of MSA-regulated genes were identified, we decided to cross-reference the MSA-regulated genes list with existing prostate cancer microarray data sets to help prioritizing biomarker candidates (Fig. 1a). Of the 809 genes regulated by MSA, 80 genes were also found among the 869 genes we previously identified to display significantly decreased expression in prostate tumors compared with normal prostate tissue². Five of the 80 genes were found among the 273 genes we previously identified whose expression is induced by treatment of prostate cancer cell lines with the DNA methyltransferase inhibitor 5-Aza-2'-deoxycytidine (5-aza-dC)³. Furthermore, SLPI (Secretory Leukocyte Peptidase Inhibitor) is the only gene that encodes for a secreted protein. We decided to further study the expression of this protein in prostate. Using immunohistochemistry, we measured the expression of SLPI in 23 normal prostate and 15 prostate tumor samples. These samples were represented by 1.5 mm cores on a tissue microarray assembled in the course of an other research project. Although not statistically significant ($p=0.12$, X² test), we observed a trend toward a diminution of expression of SLPI in cancerous tissues compared to normal tissues (Fig. 1b). To more directly characterize the effect of SLPI expression on prostate cancer cell growth, we have build a plasmid construct directing its expression. Prostate cancer cells are transfected with the plasmid construct to assess the resulting phenotype. These experiments are currently carried out.

Key research accomplishments

1. A list of potential secretory biomarkers for selenium action has been generated using bioinformatics approaches and datasets of selenium-modulated transcripts and membrane bound and secretory proteins. It provides the basis for further validation of these candidates using traditional methods.
2. The global gene expression changes induced by MSA have been assessed. The effects of MSA on cell cycle progression have been examined using bioinformatics tools and flow cytometry. MSA caused G0/G1 accumulation of the cells. The effects of MSA on androgen-regulated gene expression have been determined.
3. The number of potential biomarker candidates has been narrow down by cross-referencing with existing prostate cancer microarray data sets.
4. For one biomarker candidate, we have assessed its expression in prostate tissue and started the functional studies.

Reportable outcomes

1. Published papers

Title: Diverse effects of methylseleninic acid on the transcriptional program of human prostate cancer cells.

Authors: Zhao H, Whitfield ML, Xu T, Botstein D, Brooks JD.

Journal: *Mol Biol Cell*. 2004 Feb;15(2):506-19.

Title: Genome-wide characterization of gene expression variations and DNA copy number changes in prostate cancer cell lines.

Authors: Zhao H, Kim Y, Wang P, Lapointe J, Tibshirani R, Pollack JR, Brooks JD.

Journal: *Prostate* 2005. May 1;63(2):187-97

Title: Molecular targets of doxazosin in human prostatic stromal cells.

Authors: Zhao H, Lai F, Nonn L, Brooks JD, Peehl DM.

Journal: *Prostate* 2005. Mar 1;62(4):400-10

2. Training completed

AACR Pathobiology of Cancer - The Edward A. Smuckler Memorial Workshop
Workshop 2004, July Snowmass Village, Colorado

Conclusions

1. A subset of genes that show expression changes after selenium supplementation encode secretory proteins. These proteins may be detected in serum and serve as biomarkers of response to selenium.
2. Our results suggest that MSA may protect against prostate cancer by inhibiting cell proliferation, by modulating the expression of AR, and AR-regulated genes and by inducing carcinogen defenses.

References

1. Zhao, H., Whitfield, M. L., Xu, T., Botstein, D. & Brooks, J. D. Diverse effects of methylseleninic acid on the transcriptional program of human prostate cancer cells. *Mol Biol Cell* **15**, 506-19 (2004).
2. Lapointe, J. et al. Gene expression profiling identifies clinically relevant subtypes of prostate cancer. *Proc Natl Acad Sci U S A* (2004).
3. Kim, H. et al. The retinoic acid synthesis gene ALDH1a2 is a candidate tumor suppressor in prostate cancer. *Cancer Res.* **65**, 8118-24. (2005).

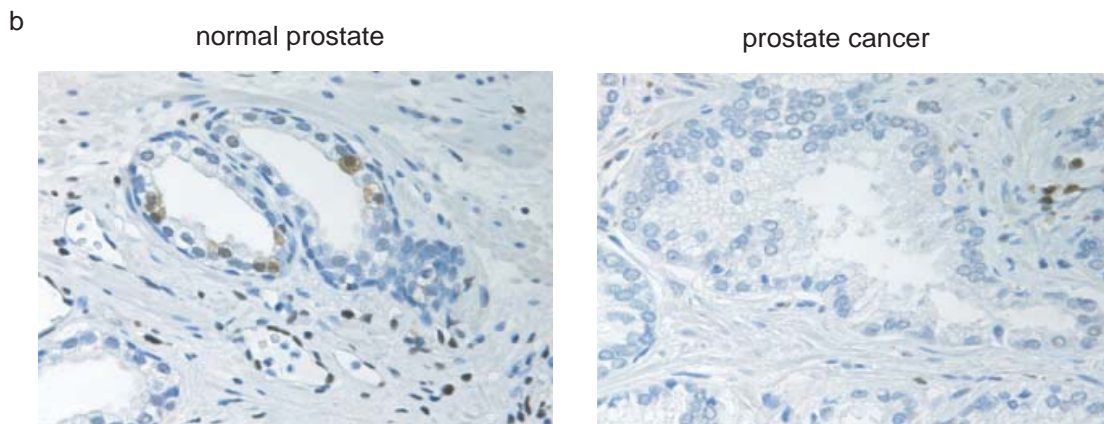
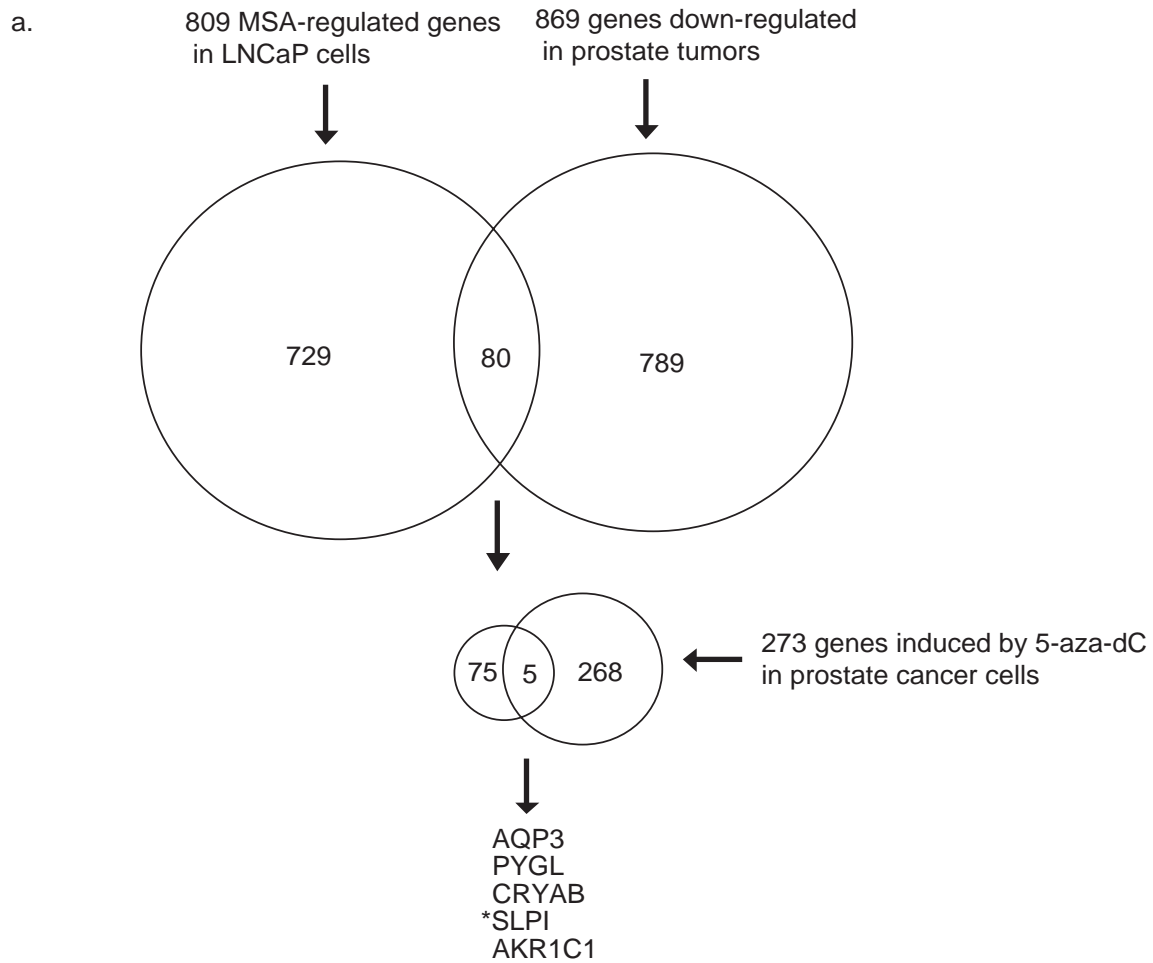


Figure 1. Identification of SLPI as a potential biomarker of selenium action. **a**, flow diagram depicting the cross-referencing of selenium modulated genes with other microarray data sets to identify *SLPI* as a relevant biomarker candidate of selenium (see text for details). **b**, Immunohistochemistry staining of normal and prostate cancer tissues with anti *SLPI* antibody.

Diverse Effects of Methylseleninic Acid on the Transcriptional Program of Human Prostate Cancer Cells

Hongjuan Zhao,* Michael L. Whitfield,[†] Tong Xu,[‡] David Botstein,[†] and James D. Brooks*[§]

Departments of *Urology, [†]Genetics, and [‡]Hematology, Stanford University School of Medicine, Stanford, California 94305

Submitted July 17, 2003; Revised October 14, 2003; Accepted October 17, 2003
Monitoring Editor: Keith Yamamoto

Methylseleninic acid (MSA) has been shown to have potent anticancer activity and is an excellent compound for studying the anticancer effects of selenium in vitro. To gain insights into the effects of MSA in prostate cancer, we characterized the global transcriptional response of LNCaP, an androgen-sensitive human prostate cancer cell line, to MSA by using high-density cDNA microarrays. We identified 951 genes whose expression shows striking dose- and time-dependent changes in response to 3–30 μ M MSA over the time course of 48 h. Transcript levels of many cell cycle-regulated genes change in response to MSA, suggesting that MSA inhibits proliferation. Consistent with these gene expression changes, cell proliferation, monitored by carboxyfluorescein succinimidyl ester staining, was decreased after MSA treatment, and an accumulation of cells at G0/G1 phase was detected by flow cytometry. Surprisingly, MSA also modulated expression of many androgen-regulated genes, suppressed androgen receptor (AR) expression at both mRNA and protein level, and decreased levels of prostate specific antigen secreted into the medium. Low concentrations of MSA also induced significant increases in transcript levels of phase 2 detoxification enzymes and induced NADPH dehydrogenase, quinone 1 enzymatic activity, a surrogate marker of global phase 2 enzyme activity. Our results suggest that MSA may protect against prostate cancer by inhibiting cell proliferation, by modulating the expression of AR and AR-regulated genes and by inducing carcinogen defenses.

INTRODUCTION

Increasing evidence suggests that selenium compounds have promise as prostate cancer preventive agents. Several epidemiological studies have shown an inverse association between selenium levels in the serum or toenails and the subsequent risk of developing prostate cancer (Willett *et al.*, 1983; Yoshizawa *et al.*, 1998; Helzlsouer *et al.*, 2000; Nomura *et al.*, 2000; Brooks *et al.*, 2001a). Animal and human intervention trials have shown that a daily supplementation with selenium-containing compounds reduces the risk of several malignancies, particularly human prostate cancer (Ip and White, 1987; el-Bayoumy, 1994; Reddy *et al.*, 1994; Clark *et al.*, 1996, 1998; Medina *et al.*, 2001; Rao *et al.*, 2001; Davis *et al.*, 2002; Duffield-Lillico *et al.*, 2002). The Nutritional Prevention of Cancer Trial, for instance, showed significantly lower incidence of prostate cancer diagnosis in subjects randomized to receive 200 μ g of selenized yeast after 6.4 and 7.4 yr of follow-up, as well as reduced total cancer incidence (Clark *et al.*, 1996; Duffield-Lillico *et al.*, 2002). Although this study has been criticized for its use of secondary endpoints, it has

provided compelling rationale for the recently initiated Selenium and Vitamin E Cancer Prevention Trial (SELECT), a 12-year prospective, randomized trial involving 32,000 men (Hoque *et al.*, 2001; Klein *et al.*, 2001).

The inverse relationship between selenium intake and prostate cancer risk has prompted a great deal of interest in understanding the mechanisms of selenium chemoprevention. Diverse forms of selenium have been shown to affect a variety of biological processes important in carcinogenesis (Ip, 1998; Combs, 2001; El-Bayoumy, 2001; Fleming *et al.*, 2001; Ganther, 2001; Kim and Milner, 2001; Lu and Jiang, 2001; Youn *et al.*, 2001). Selenium compounds have been shown to inhibit cell proliferation and induce apoptosis, and these are thought to be major mechanisms by which selenium prevents tumor initiation or progression (Ip *et al.*, 2000a; Combs, 2001; Ganther, 2001; Lu, 2001). Selenium compounds also protect cells against oxidative stress and genetic damage, and block tumor angiogenesis (El-Bayoumy, 2001; Lu and Jiang, 2001). However, a comprehensive understanding of the mechanisms underlying selenium's anticancer effects is currently lacking.

Monomethylated forms of selenium are highly potent and efficacious chemopreventive agents. Methylselenocysteine (MSC) and methylseleninic acid (MSA) have been shown to be more active in cancer prevention than inorganic selenite, or selenomethionine, the form of selenium being used in SELECT (Ip *et al.*, 1991; Ip, 1998; Combs, 2001; Hoque *et al.*, 2001; Klein *et al.*, 2001). It is believed that they are the direct precursors of methylselenol, possibly the key metabolite responsible for selenium's anticancer activity. Whereas MSC

Article published online ahead of print. Mol. Biol. Cell 10.1091/mbc.E03-07-0501. Article and publication date are available at www.molbiolcell.org/cgi/doi/10.1091/mbc.E03-07-0501.

[§] Corresponding author. E-mail address: jdbrooks@stanford.edu.
Abbreviations used: AR, androgen receptor; CFSE, carboxyfluorescein succinimidyl ester; GAPDH, glyceraldehyde-3-phosphate dehydrogenase; MSA, methylseleninic acid; MSC, methylselenocysteine; NQO1, NADPH dehydrogenase, quinone 1; PSA, prostate-specific antigen.

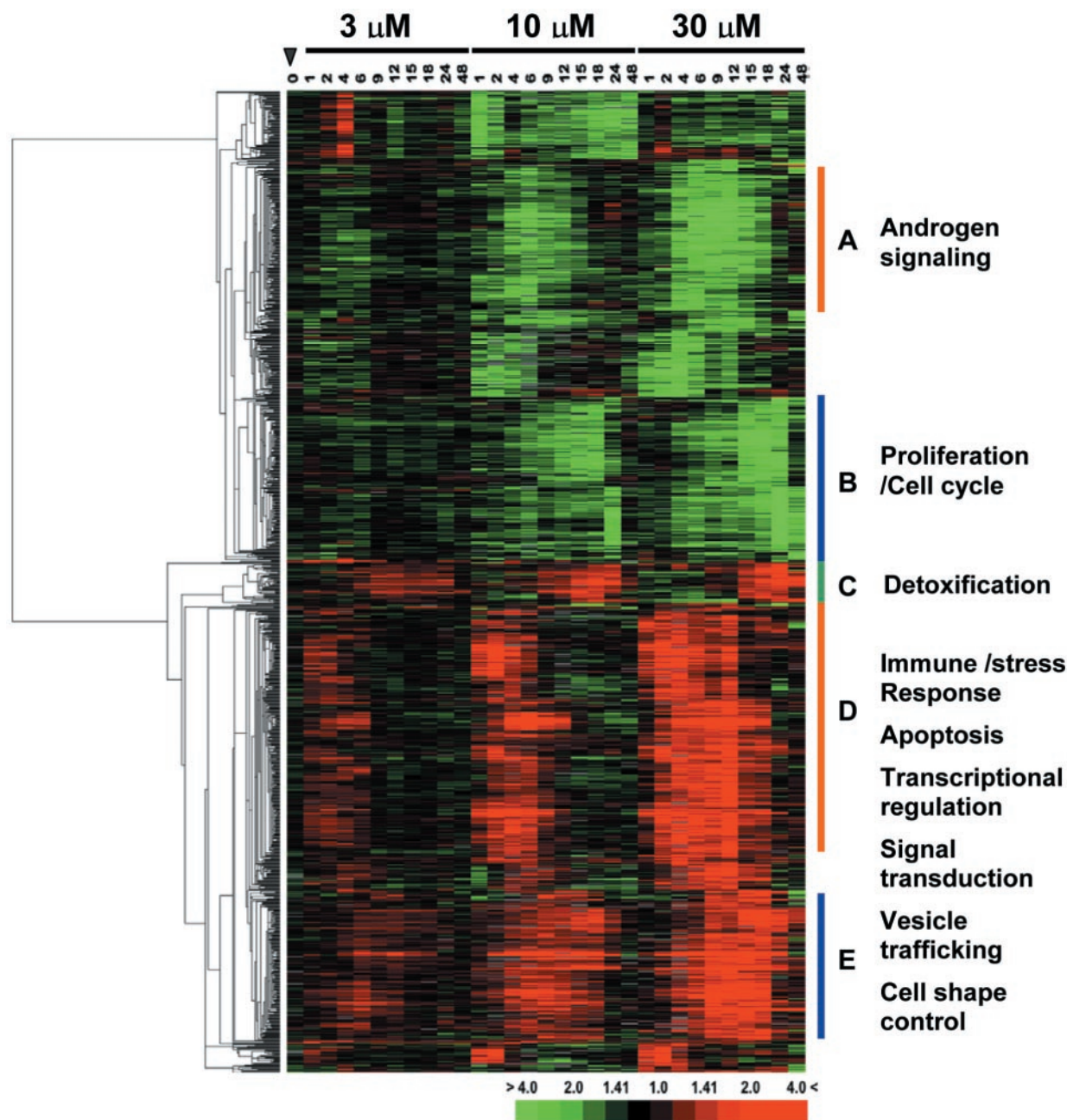


Figure 1. Hierarchical clustering analysis of MSA-responsive genes in LNCaP cells. Each column represents data from a single time point after treatment with MSA, and each row represents expression levels for a single gene across the time course. The 1128 transcripts were up-regulated (red) or down-regulated (green) after exposure to 3, 10, or 30 μM MSA as indicated at the top of the image. The degree of color saturation corresponds with the ratio of gene expression shown at the bottom of the image. For comparison, the gene expression pattern of untreated cells at time 0 is shown at the closed arrowhead. The data from each treatment condition were arranged in a time ascending order (1, 2, 4, 6, 9, 12, 15, 18, 24, and 48 h) as indicated on top of the image. The gene tree shown at the left of the image corresponds to the degree of similarity (Pearson correlation) of the pattern of expression for genes across the experiments. Genes in cluster A–E show different temporal response to MSA in a dose-dependent manner. Full transcript identities and raw data are available at <http://www.Stanford.edu/~hongjuan/MSA>.

requires the action of cysteine conjugate β -lyase or related lyases to be converted to methylselenol, MSA does not (Andreadou *et al.*, 1996; Ganther and Lawrence, 1997; Ip, 1998; Ip *et al.*, 2000b). It is 10 times more potent than MSC in affecting biological processes *in vitro*, probably because of limited β -lyase activity in cultured eukaryotic cells (Ip *et al.*, 2000b).

Therefore, MSA is an ideal compound for studying the anticancer effects of selenium *in vitro*.

DNA microarrays provide a genome-wide view of the biological processes affected by cellular perturbations and offer an opportunity to gain new insights into the mechanisms by which preventive agents exert their effects (Wil-

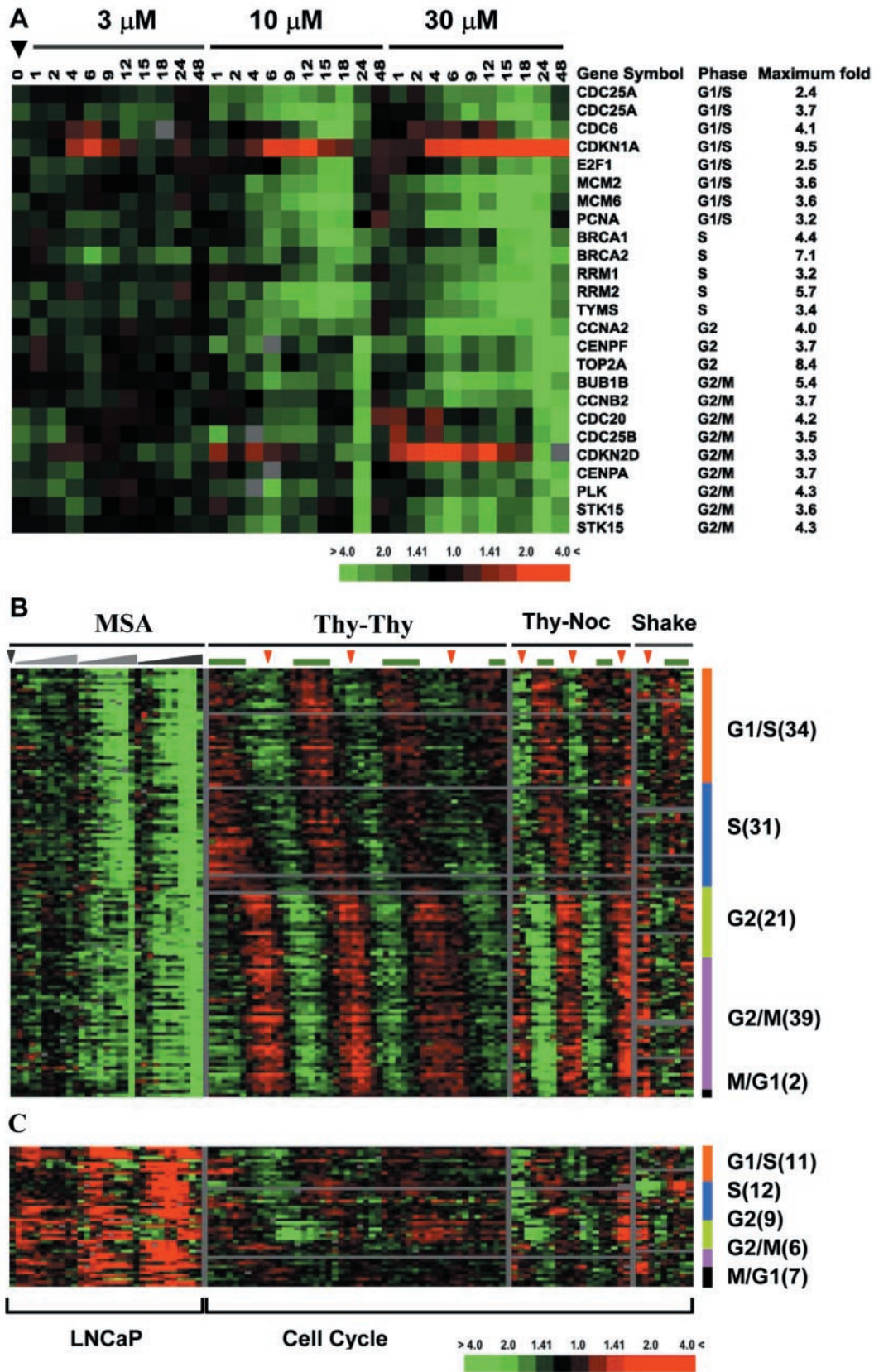


Figure 2. Cell cycle-regulated genes modulated by MSA. Genes that occur more than once are represented by multiple clones on arrays. (A) Transcripts representing previously characterized cell cycle-regulated genes. (B) Cell cycle-regulated transcripts identified by Whitfield *et al.* (2002) that are down-regulated by MSA. The number of transcripts belonging to different cell cycle phases is shown at the right of the image.

liams and Brooks, 2001). Herein, we have undertaken a systematic evaluation of the changes in gene expression that result from treatment of the androgen-sensitive prostate cancer cell line LNCaP with MSA. We identified 1128 clones representing 951 genes whose expression levels are affected by MSA in a time- and dose-dependent manner. The transcriptional profiles and confirmatory experiments suggest that MSA causes cell accumulation at G0/G1 modulates the expression of androgen receptor (AR) and its regulated genes, and induces enzymes that detoxify carcinogens.

MATERIALS AND METHODS

Cell Culture and Treatment

LNCaP cells were cultured in RPMI 1640 medium with 2 mM L-glutamine, 100 U/ml penicillin/100 µg/ml streptomycin (Invitrogen, Carlsbad, CA), and 5% defined fetal bovine serum that contributed 13 nM selenium to the medium (Hyclone Laboratories, Logan, UT). When cells reached ~40–60% confluence, the medium was changed, and 12–24 h later the cells were treated with 3, 10, or 30 µM MSA (pH adjusted to 7.0) (Selenium Technologies, Lubbock, TX). The doses used in this study were chosen based on previous studies using MSA in vitro and reported selenium levels in human serum (Ip *et al.*, 2000b; Nomura *et al.*, 2000; Brooks *et al.*, 2001a; Jiang *et al.*, 2001; Sinha *et al.*, 2001; Dong *et al.*, 2002; Zhu *et al.*, 2002). At several time points after exposure, total RNA was harvested as described below. Untreated cells cultured in parallel were used as controls for each time point.

Total RNA Isolation

Medium was aspirated from each 150-mm cell culture plate, and 5 ml of TRIzol solution (Invitrogen) was added. After 5 min of gentle agitation, lysates were extracted with chloroform, and the organic and aqueous layers were separated using Phase Lock Gel (Eppendorf-5 Prime, Inc., Boulder, CO). Total RNA was precipitated with isopropanol and further purified with RNeasy mini kit (QIAGEN, Valencia, CA). The concentration of total RNA was determined using an MBA 2000 spectrometer (PerkinElmer Life Sciences, Boston, MA), and the integrity of total RNA was assessed using a 2100 Bioanalyzer (Agilent Technologies, Palo Alto, CA).

cDNA Microarray Hybridizations

Fluorescently labeled cDNA probes were prepared from 70 µg of total RNA isolated from MSA-treated cells (Cy5 labeled) and control cells (Cy3 labeled) by reverse transcription with an Oligo dT primer 5'-TTTTTTTTTTTTTTT-3' (QIAGEN) as described previously (Zhao *et al.*, 2002). Labeled probes from MSA-treated and control cells for each time point were mixed and hybridized overnight to spotted cDNA microarrays with 42,941 elements (Stanford Functional Genomics Facility). Microarray slides were then washed to remove unbound probe and analyzed as described previously (Zhao *et al.*, 2002).

Data Processing and Analysis

Fluorescence intensities for each fluorophore were acquired using an Axon scanner 4000B and analyzed with GenePix Pro3.0 software (Axon Instruments, Union City, CA). Spots of poor quality were removed from further analysis by visual inspection. Data files containing fluorescence ratios were entered into the Stanford Microarray Database where biological data were associated with fluorescence ratios, and genes were selected for further analysis (Sherlock *et al.*, 2001). Only spots with a signal intensity >150% above background in both Cy5 and Cy3 channels in at least 80% of the microarray experiments were used in the subsequent analysis. We arbitrarily selected transcripts whose expression level varied at least twofold after treatment compared with controls in at least three of the experiments examined. Prior work has shown that twofold variations in expression reliably reflect changes in expression levels measured by other methods (Blader *et al.*, 2001; Jones and

Arvin, 2003). The genes in the resulting data table were ordered by their patterns of gene expression by using hierarchical clustering analysis (Eisen *et al.*, 1998) and visualized using Treeview software (<http://rana.lbl.gov/Eisen-Software.htm>). The data for all 1128 clones as well as the primary data are available at <http://www.stanford.edu/~hongjuan/MSA>.

Cell Proliferation and Cell Cycle Assay

Cell proliferation was determined using 5- or 6-(N-succinimidylsuccinyl)-3',6'-O,O'-diacetylfluorescein (CFSE) (Dojindo Molecular Technologies, Gaithersburg, MD) staining (Lyons, 2000; Groszer *et al.*, 2001). Untreated cells were stained with 1 µM CFSE in RPMI 1640 medium at 37°C for 10 min before being seeded in 60-mm plates with fresh media. After cells were cultured overnight, the media were again changed to eliminate residual CFSE that may have leaked from the cells. Half of the plates were treated with MSA for different lengths of time and harvested by trypsinization, and the remaining untreated plates cultured in parallel were used as controls. The absolute intensity of CFSE within each cell was measured by flow cytometry, and the average intensity of CFSE within the population calculated using Flow Jo software (<http://www.flowjo.com/v4/html/overview.html>).

Cell cycle distribution was determined by propidium iodide (PI) (Sigma-Aldrich, St. Louis, MO) staining. After aspirating the media, treated and control cells were collected by trypsinization and washed with 1× phosphate-buffered saline. Duplicate samples were collected for each growth condition. Cells were fixed with 70% ice-cold ethanol overnight and stained with PI (20 µg/ml) in presence of RNase A (300 µg/ml) at 37°C for 30 min. The DNA content of the cells was determined by flow cytometry, and cell cycle distribution was analyzed with Flow Jo software.

Western Blotting

Treated and control cells were lysed with 1 ml of radioimmunoprecipitation assay buffer (pH 7.4, 50 mM Tris-HCl, 1% NP-40, 0.25% Na-deoxycholate, 150 mM NaCl, 1 mM EDTA, 1 mM phenylmethylsulfonyl fluoride, 1 µg/ml aprotinin). The cell lysate was passed through a 21-gauge needle to shear the cellular DNA. Protein concentration was determined using a BCA protein assay kit (Pierce Chemical, Rockford, IL). Ten to 15 µg of protein was separated using a 4–20% Tris-HCl precast gel (Bio-Rad, Hercules, CA), and transferred to a Hybond-P membrane (Amersham Life Sciences, Arlington Heights, IL). AR was detected with a rabbit polyclonal antibody against the amino terminus of human AR, sc-816 (Santa Cruz Biotechnology, Santa Cruz, CA) and visualized with an ECL Plus kit (Amersham Biosciences, Piscataway, NJ). Glyceraldehyde-3-phosphate dehydrogenase (GAPDH) was detected with a monoclonal mouse anti-rabbit antibody, MoAb 6C5, which reacts with human GAPDH (Research Diagnostics, Flanders, NJ). AR and GAPDH signal intensities were quantified with a GS-700 densitometer (Bio-Rad).

Determination of Secreted Prostate-specific Antigen (PSA) Levels

Media from MSA-treated and control cells cultured on a 24-well plate was aspirated and stored at –80°C. PSA concentration in the thawed medium was measured using a human prostate specific antigen ELISA kit (Alpha Diagnostic International, San Antonio, TX) and was normalized to total protein of cells cultured in the same well where the medium was taken.

NADPH Dehydrogenase, Quinone 1 (NQO1) Enzymatic Activity Assay

After aspirating the media, treated and control cells cultured in a 96-well plate were lysed with 200 µl of 0.08% digitonin (Sigma-Aldrich)/2 mM EDTA (pH 8.0) at 37°C for 30 min. NQO1 enzymatic activity was assessed in triplicate by the menadione-coupled reduction of tetrazolium dye as described previously (Brooks *et al.*, 2001b). Enzymatic activity for each sample was averaged across the triplicate and normalized to total cell protein in each sample.

RESULTS

MSA Affects Gene Expression in LNCaP Cells in a Dose- and Time-dependent Manner

To study systematically the effects of MSA in human prostate cancer cells in vitro, we characterized the temporal program of gene expression induced by treating LNCaP cells with three different concentrations of MSA. Thirty-one samples (10 samples/concentration over the course of 48 h plus one sample from untreated cells) were analyzed on microarrays containing ~42,941 features representing ~29,587 different human genes as inferred from UNIGENE clusters. The 1128 clones representing 951 genes displayed changes in expression levels of at least twofold after MSA treatment compared with controls in at least three samples.

Figure 2 (cont). The effect of MSA on expression of these genes is shown to the left organized in the same order as in A. The pattern of these genes across multiple cell cycles in HeLa cells is shown to the right. Thy-Thy indicates a double thymidine block to synchronize cells at S phase before release. Thy-Noc indicates a thymidine-nocodazole block to synchronize cells at mitosis before release. Shake indicates cells collected with an automated cell shaker that were used as synchronized in mitosis. The green bar above each column represents S phase, and the red arrowheads indicate mitosis as estimated by flow cytometry or bromodeoxyuridine labeling. (C) Cell cycle-regulated transcripts identified by Whitfield *et al.* (2002) that are up-regulated by MSA.

Many of the transcripts represent poorly characterized genes or expressed sequence tags. The data for the 1128 transcripts were ordered by their patterns of gene expression by hierarchical clustering (Eisen *et al.*, 1998) (Figure 1). The complete data set, including raw data, is available at <http://www.stanford.edu/~hongjuan/MSA>.

MSA produced discrete, reproducible, time- and dose-dependent changes in gene expression in LNCaP cells. Expression changes were largely similar among cells treated with 3, 10, and 30 μ M MSA; however, with higher concentrations of MSA, changes in gene expression were larger in both the magnitude and duration. The number of transcripts whose expression increased or decreased was similar (541 and 587, respectively). Approximately one-half of the transcripts showed changes within 1–2 h after treatment with peak variation occurring within 8 h and returned to baseline expression levels by 24 h (Figure 1, clusters A and D). Many of the functionally characterized genes in cluster A are known to be involved in androgen signaling pathways. The remaining transcripts were delayed in their response, with expression changes that peaked between 12 and 24 h and that remained apparent at 48 h (Figure 1, clusters B, C, and E). These included genes involved in cell cycle regulation (cluster B) and phase 2 detoxification enzymes (cluster C). Known genes in clusters D and E are involved in diverse biological processes, including immune and stress responses (IGSF3, IGSF4, and NFIL3), apoptosis regulation (BIRC2, BIRC3, and TNFAIP3), transcriptional regulation (ATF3, ELF3, and MAD), signal transduction (JAK1, ARHB, and SH3BP5), tumor suppression (MEN1, ING1, and IRF1), vesicle trafficking (SEC24D, STX1A, and RAB31), and cell shape control (KLHL2, WASF1, and MAP1B).

MSA Changes Expression of Cell Cycle-regulated Genes

MSA has been shown to inhibit cell growth through its effects on the cell cycle in several model systems, although not in the LNCaP cell line. A subset of the 1128 transcripts (Figure 1, cluster B) modulated by MSA in LNCaP cells represent known cell cycle-regulated genes (Figure 2A). To gain insight into the effect of MSA on cell cycle-regulated genes, we compared these 1128 transcripts to a set of 1134 transcripts (representing >850 genes) that vary periodically as synchronized HeLa cells pass through the cell cycle (Whitfield *et al.*, 2002). In the latter data set, all 1134 transcripts were grouped according to the phase in the cell cycle where their expression peaked. Between the MSA and cell cycle data sets, 172 transcripts were found in common. The 127 transcripts that showed decreased expression were distributed throughout all phases of the cell cycle and included genes involved in DNA replication initiation (CDC6, MCM2, and MCM6), DNA repair (PCNA), and cell cycle control (CDC25A and E2F1) expressed in G1/S phase, DNA replication (RRM1, RRM2, and TYMS) expressed in S phase, chromosome condensation and organization (TOP2A and CENPA), mitotic spindle checkpoint (CDC20 and BUB1B), and centrosome duplication (PLK and STK15) expressed in G2 and M phase (Figure 2B). There were 45 clones in common between the data sets that were up-regulated by MSA that, again, were distributed throughout all phases of the cell cycle. These transcripts show periodic expression in HeLa cells with an expression pattern that was the inverse of the genes that are down-regulated by MSA. In this set of transcripts are known inhibitors of proliferation, most notably CDKN1A (p21), CDKN2D (p19), and CDKN1C (p57), all of which are potent negative regulators of G1 cyclin/cdk complexes (Sherr and Roberts, 1999; Gitig and Koff, 2000). This

suggests that induction of this set of genes by MSA may modulate decreased proliferation in LNCaP cells.

The distribution of transcripts affected by MSA across all phases of the cell cycle suggested that MSA might cause LNCaP cells to exit the cell cycle, rather than induce an arrest at a specific cell cycle phase or slow cell cycle progression. In the HeLa cell cycle experiments, cell cycle arrest was associated with high expression of transcripts typically expressed during the phase of the cell cycle at which arrest occurs (see Thy-Thy, Thy-Noc, and Shake off in Figure 2B). In LNCaP treated with MSA, on the other hand, expression variations of cell cycle-regulated transcripts were not selectively associated with any particular phase of the cell cycle; cell cycle-regulated transcripts typically expressed in a particular phase of the cell cycle (i.e., G1, S, or G2/M) all showed decreased expression and the transcripts that displayed increased expression are known to inhibit cell proliferation. These expression changes, therefore, suggest that cells are exiting the cell cycle in response to MSA, rather than arresting at a particular phase in the cell cycle.

MSA Inhibits Cell Proliferation by Induction of Cell Accumulation at G0/G1

Based on the expression changes in the cell cycle-regulated genes, we assessed the effect of MSA on the proliferation of the LNCaP cells after pulse exposure to CFSE. CFSE diffuses freely into cells where it is converted to a fluorescently tagged membrane impermeable dye that is retained in the cytoplasm. With each round of cell division, the retained CFSE is partitioned equally to daughter cells and the relative intensity of the dye becomes decreased by half. At concentrations between 3 and 30 μ M, MSA produced a dose-dependent inhibition of LNCaP cell growth, evident by the significantly higher mean intensity of CFSE in treated cells compared with controls (Figure 3). CFSE levels in MSA-treated cells remained high relative to control cells up to 48 h and then the inhibitory effect began to diminish (our unpublished data). Exchange of the medium at 72 h and retreatment with MSA produced growth inhibition out to 120 h similar in magnitude to that produced by the first treatment. Therefore, as predicted from gene expression profiling, MSA inhibits LNCaP cell growth and cells retain sensitivity to this inhibition with repeated treatments.

To evaluate whether the decreased proliferation we observed was most consistent with cell cycle arrest or exit from the cell cycle, we performed flow cytometry on MSA-treated and untreated LNCaP cells. The proportion of cells at G0/G1, S, and G2/M phase was determined after 24-h exposure to different concentrations of MSA. Cells treated with 3, 6, 10, and 30 μ M MSA all showed an increase in the percentage of cells at G0/G1 phase with a corresponding depletion of cells in S and G2/M phase (Figure 4). The most pronounced effects were seen with 6 and 10 μ M MSA, where the fraction of cells in S and G2/M phase decreased by 66 and 63%, respectively. We did not see evidence of apoptosis at any of the doses tested. These results are most consistent with MSA inducing either G1 arrest or causing cells to exit the cell cycle (G0).

MSA Modulates Transcript Levels of AR and Androgen-responsive Genes

To our surprise, we found that MSA modulated the expression of AR and a group of well-characterized androgen-regulated genes in a time- and dose-dependent manner. Two clones representing AR showed decreased

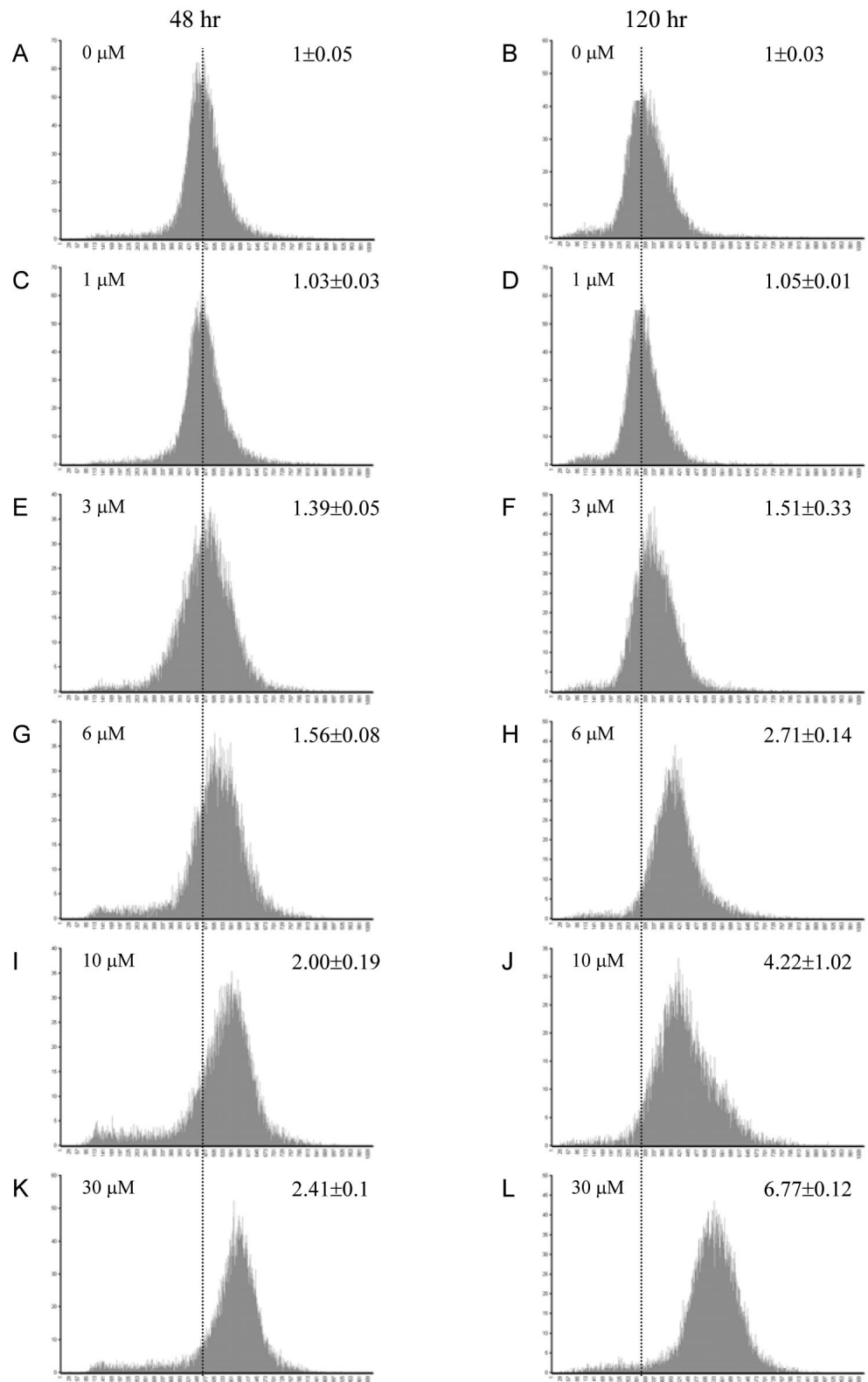


Figure 3. Cell proliferation monitored by CFSE staining and flow cytometry with and without MSA exposure. The y-axis represents the number of cells, and the x-axis represents the intensity of CFSE in the cells. Cells harvested 48 h after CFSE staining (left) and 120 h (right). Media with fresh MSA were exchanged at 72 h after CFSE staining. The concentration of MSA used to treat the cells is shown at the top left corner of each graph. The mean average intensity of CFSE in treated cells was normalized against that of the control cells and is shown at the top right corner of each graph. Each graph represents data from triplicate samples.

transcript levels in response to MSA, and 19 known androgen-regulated genes showed altered transcript levels. MSA suppressed expression of 12 androgen-induced genes (KLK3, KLK2, ACPP, NKX3A, TMPRSS2, E2F1, ARSDR1, FKBP5, TUBA2, TUBB2, PPFIA1, and AIBZIP) and

increased expression of six of seven genes normally suppressed by androgen (APOD, CLU, PEG3, UGD, NDRG1, and SERPINB5) (Figure 5A). Myc transcript levels, previously shown to be suppressed by androgen, showed a biphasic response to MSA.

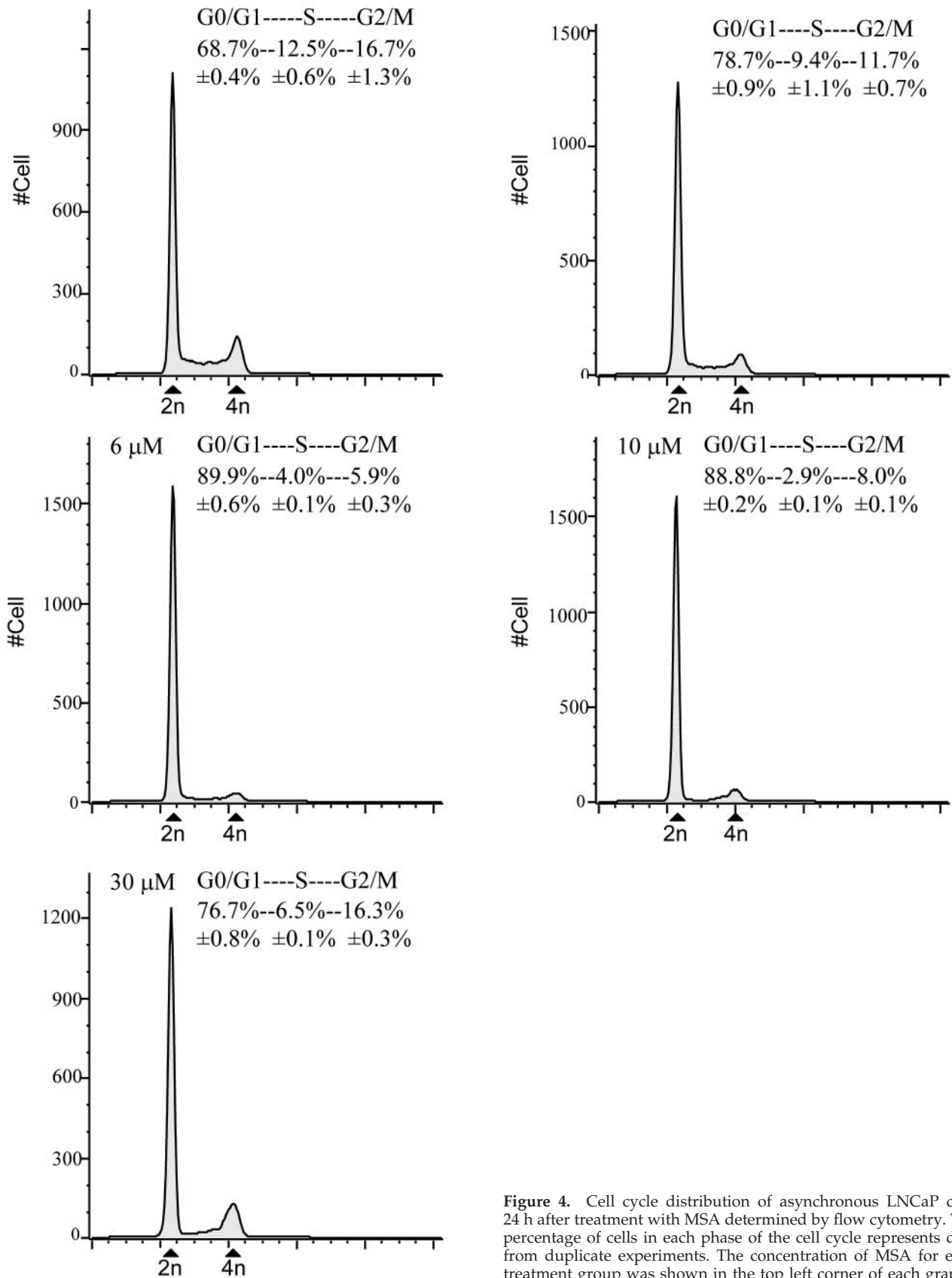


Figure 4. Cell cycle distribution of asynchronous LNCaP cells 24 h after treatment with MSA determined by flow cytometry. The percentage of cells in each phase of the cell cycle represents data from duplicate experiments. The concentration of MSA for each treatment group was shown in the top left corner of each graph.

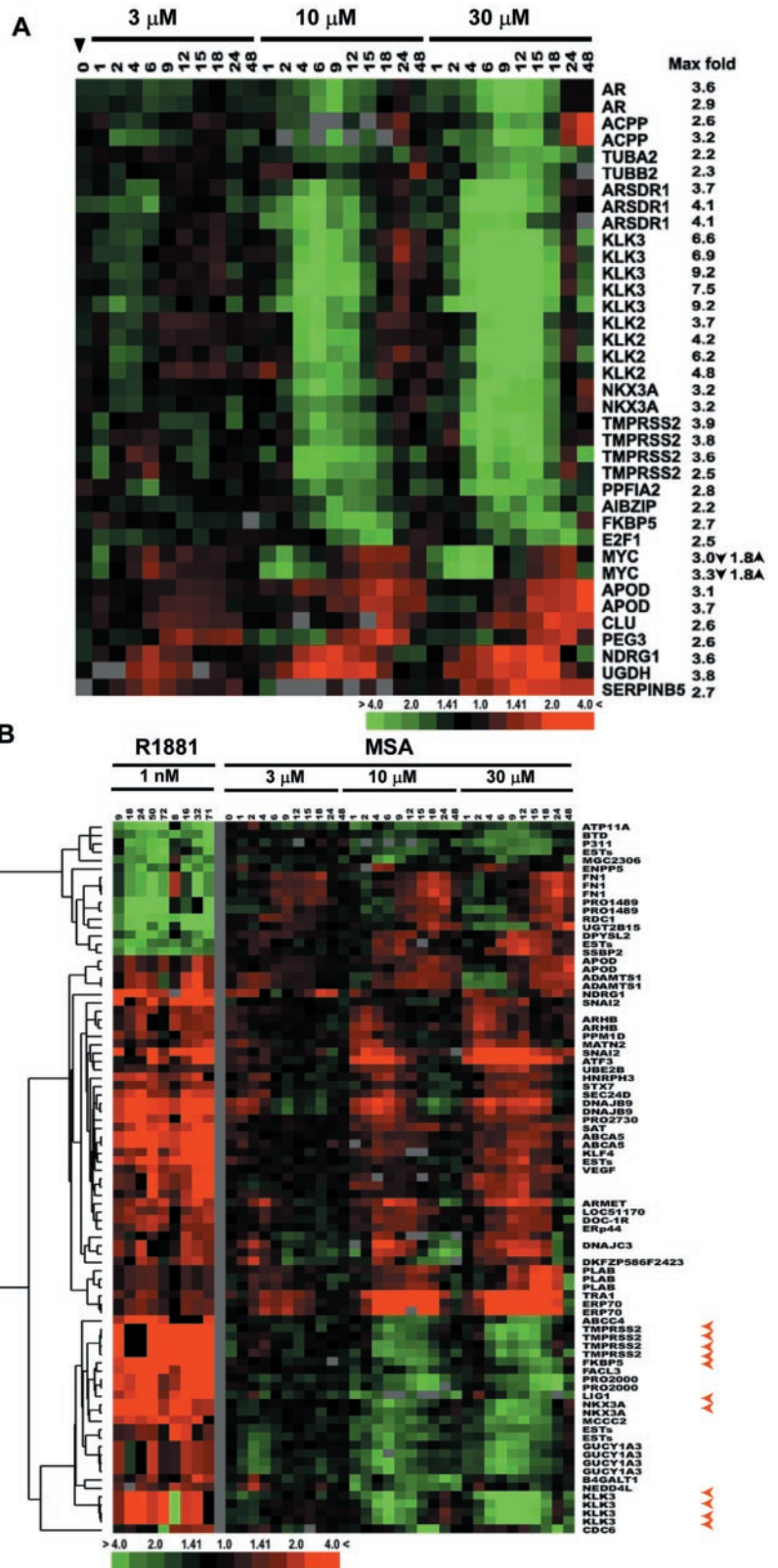


Figure 5. Androgen-responsive genes modulated by MSA. Genes that occur more than once are represented by multiple clones on arrays. (A) MSA-induced expression changes of known androgen-regulated genes. (B) MSA-affected transcripts that are present in a list of androgen-responsive transcripts identified by DePrimo *et al.* (2002). On the left are gene expression patterns from two separate time courses induced by treatment of LNCaP cells with the synthetic androgen R1881. On the right are expression patterns of this same set of genes after MSA treatment. The red arrowheads point to well-characterized androgen-regulated genes.

We compared our MSA-regulated data set to a recently reported set of 103 androgen-regulated genes (Nelson *et al.*, 2002) and found that 18 of 26 genes found in both data sets showed a reciprocal response to MSA (Table 1). Intriguingly,

when compared with a set of 567 androgen-regulated transcripts we had identified previously (DePrimo *et al.*, 2002), 85 of the MSA-regulated transcripts representing 61 genes were found in common, and only one-half of the transcripts

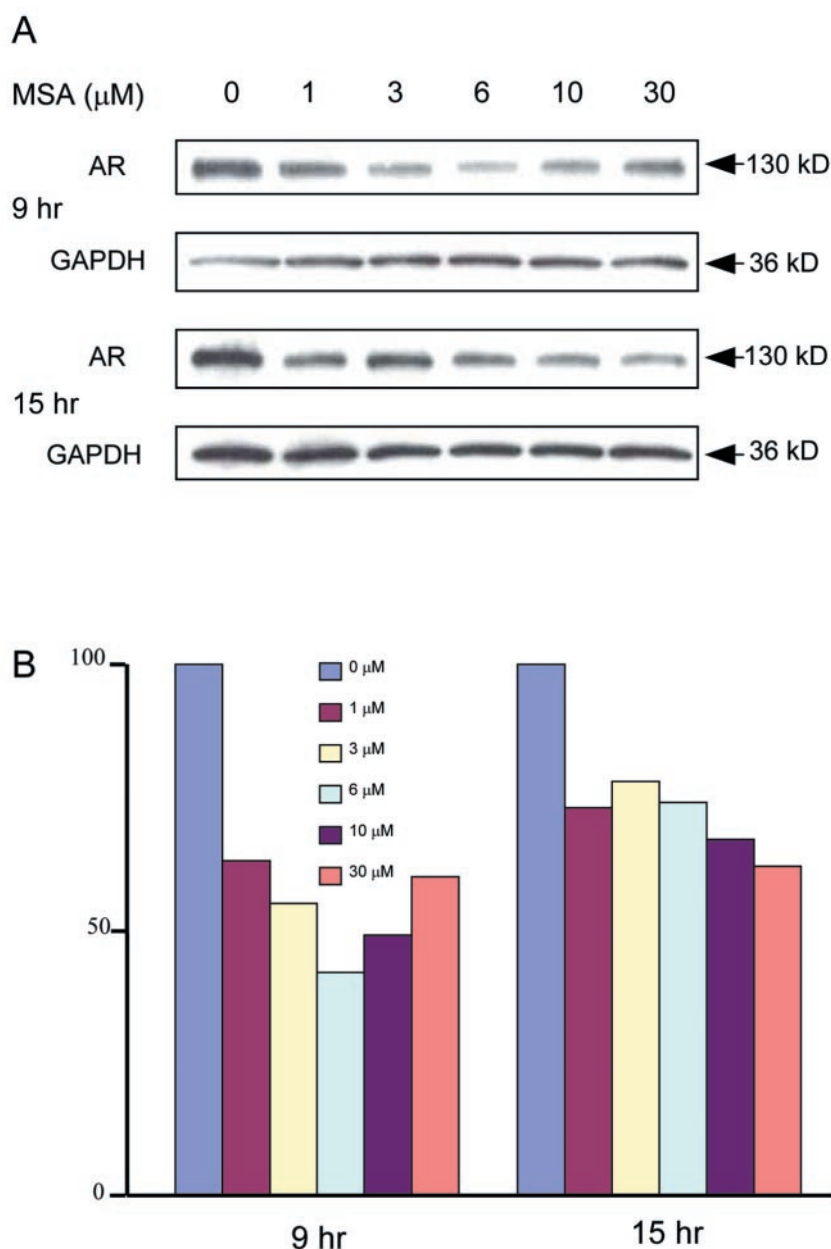


Figure 6. MSA decreases AR protein expression. (A) AR protein level after 9 and 15 h of exposure to different concentrations of MSA by western blotting analysis. GAPDH from each sample is shown as an internal control. (B) Quantitation of AR protein levels by using a densitometer. The signal intensity of AR was normalized to GAPDH in each same sample. AR intensity of treated cells was normalized against that of the untreated control cells.

were reciprocally regulated (Figure 5B). Therefore, comparison of the MSA expression data set to this larger androgen-regulated data set suggested that MSA has mixed effects on androgen-responsive genes.

MSA Represses AR Protein Expression and the Level of Secreted PSA

To characterize further the effects of MSA on the androgen axis, we performed Western blotting to compare AR protein levels from treated and untreated LNCaP cells (Figure 6A). The decreased AR transcript levels we observed on the microarrays were associated with decreased AR protein levels at 9 and 15 h after MSA exposure, even at relatively low doses (1 μM). AR protein levels decreased 40–60% after 9 h of MSA exposure, and 30–40% after 15-h exposure. There did not seem to be a significant difference in the degree of AR down-regulation for different MSA concentrations at

15 h; however, 6 μM MSA produced more striking suppression of AR protein levels at 9 h (Figure 6B).

To evaluate further the effects of MSA on androgen-regulated genes, we determined the level of secreted PSA in the cell culture media after exposure of cells to MSA (Figure 7). A dose-dependent decrease in secreted PSA level was detected within 12 h after MSA exposure and continued out to 48 h. Therefore, protein levels of PSA, a well-known androgen target, show modulation similar to that observed for transcript levels using microarray analysis.

MSA Up-Regulates Detoxification Enzymes

Phase 2 detoxification enzymes function in metabolizing and inactivating xenobiotics and toxins and thereby protect cells against carcinogens. We noted 12 transcripts representing seven genes encoding phase 2 enzymes were up-regulated by MSA (Figure 8A). The mRNA levels of NQO1, a surro-

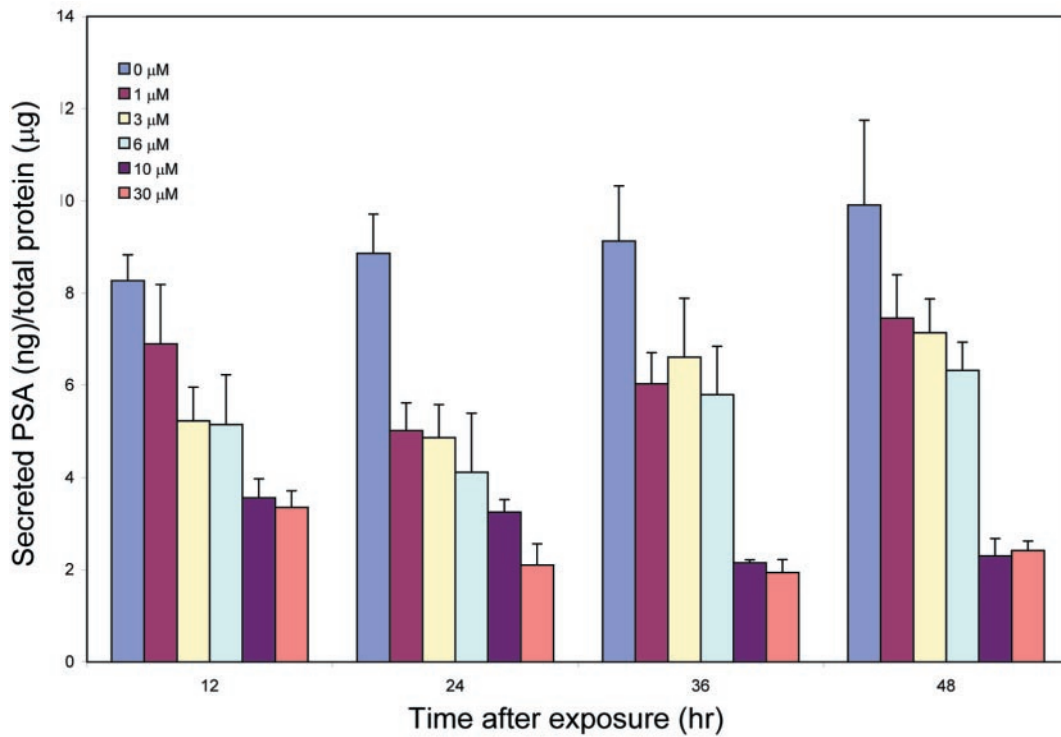


Figure 7. MSA decreases levels of PSA secreted into the media in LNCaP cells. PSA levels in the cell culture medium measured by ELISA and normalized against the total protein of the cultured cells. Each column represents data from experiments performed in triplicate.

Table 1. Comparison of gene expression changes induced by MSA and androgen reported by Nelson *et al.* (2002)

Gene symbol	Description	Expression change			Biological process
		Androgen		MSA	
		24 hr	48 hr	Max fold	
CDC14B	Cell division cycle 14 homolog B	3.0 ↑	3.1 ↑	2.9 ↓	Proliferation/differentiation/apoptosis
ID2 ^a	Hes6 neuronal differentiation gene ortholog	1.6 ↑	3.8 ↑	2.7 ↑	Proliferation/differentiation/apoptosis
NDRG1 ^b	N-myc downstream regulated	13.7 ↑	14.8 ↑	3.6 ↓	Proliferation/differentiation/apoptosis
KLK2	Kallikrein 2, prostatic	8.8 ↑	9.0 ↑	6.2 ↓	Protease/protease Inhibitor
KLK3 ^b	Kallikrein 3, prostate specific antigen	7.9 ↑	10.2 ↑	9.2 ↓	Protease/protease Inhibitor
TMPRSS2 ^b	Transmembrane protease, serine 2	15.5 ↑	18.3 ↑	3.9 ↓	Protease/protease Inhibitor
GUCY1A3 ^b	Guanylate cyclase 1, soluble, alpha 3	2.9 ↑	3.3 ↑	4.3 ↓	Signal transduction
INPP4B	Inositol polyphosphate-4-phosphatase, type II	2.3 ↑	4.6 ↑	2.3 ↓	Signal transduction
PEG3	Paternally expressed 3	3.2 ↓	4 ↓	2.6 ↑	Signal transduction
FN1 ^b	Fibronectin 1	2.5 ↓	4.4 ↓	4.1 ↑	Structure/motility/adhesion
H1FO	Histone family, member 0	2.9 ↑	3.2 ↑	7.4 ↓	Structure/motility/adhesion
B4GALT1 ^b	BetaGlcNAc beta 1,4-galactosyltransferase	3.3 ↑	3.3 ↑	3.5 ↓	Metabolism
FACL3 ^b	Fatty-acid-Coenzyme A ligase, long-chain 3	2.7 ↑	3.7 ↑	2.4 ↓	Metabolism
SAT ^a	Spermidine/spermine N1-acetyltransferase	3.7 ↑	7.3 ↑	2.3 ↑	Metabolism
SCD	Stearoyl-CoA desaturase	5.9 ↑	4.5 ↑	5.8 ↓	Metabolism
UGDH	UDP-glucose dehydrogenase	2.9 ↑	4.0 ↑	3.8 ↓	Metabolism
KLF4 ^a	Kruppel-like factor 4	2.3 ↑	3.0 ↑	2.4 ↑	Transcription regulation
MYC ^a	V-myc myelocytomatosis viral oncogene homolog	2.7 ↓	2.8 ↓	3.3 ↓ 1.8 ↑	Transcription regulation
NKX3A ^b	NK3 transcription factor homolog A (Drosophila)	14.9 ↑	14.1 ↑	3.2 ↓	Transcription regulation
ABCC4 ^b	ATP-binding cassette, sub-family C	5.5 ↑	7.8 ↑	2.5 ↓	Transport/trafficking
FKBP5 ^b	FK506 binding protein 5	24.4 ↑	25.4 ↑	2.7 ↓	Transport/trafficking
SEC24D ^{a,b}	SEC24 related gene family, member D	3.0 ↑	2.6 ↑	2.9 ↑	Transport/trafficking
RDC1 ^b	G protein-coupled receptor	7.8 ↓	4.5 ↓	2.4 ↑	Stress response
DNAJB9 ^{a,b}	Dnaj (Hsp40)homolog, subfamily B	4.0 ↑	3.6 ↑	4.2 ↑	Stress response
SGK ^a	Serum/glucocorticoid regulated kinase	4.4 ↑	2.4 ↑	2.5 ↑	Stress response
ST7 ^a	Suppression of tumorigenicity 7	2.7 ↓	4.2 ↓	2.5 ↓	Other functions

^a Genes show similar expression changes under the influence of androgen and MSA.

^b Genes that are also represented in dataset from DePrimo *et al.* (2002).

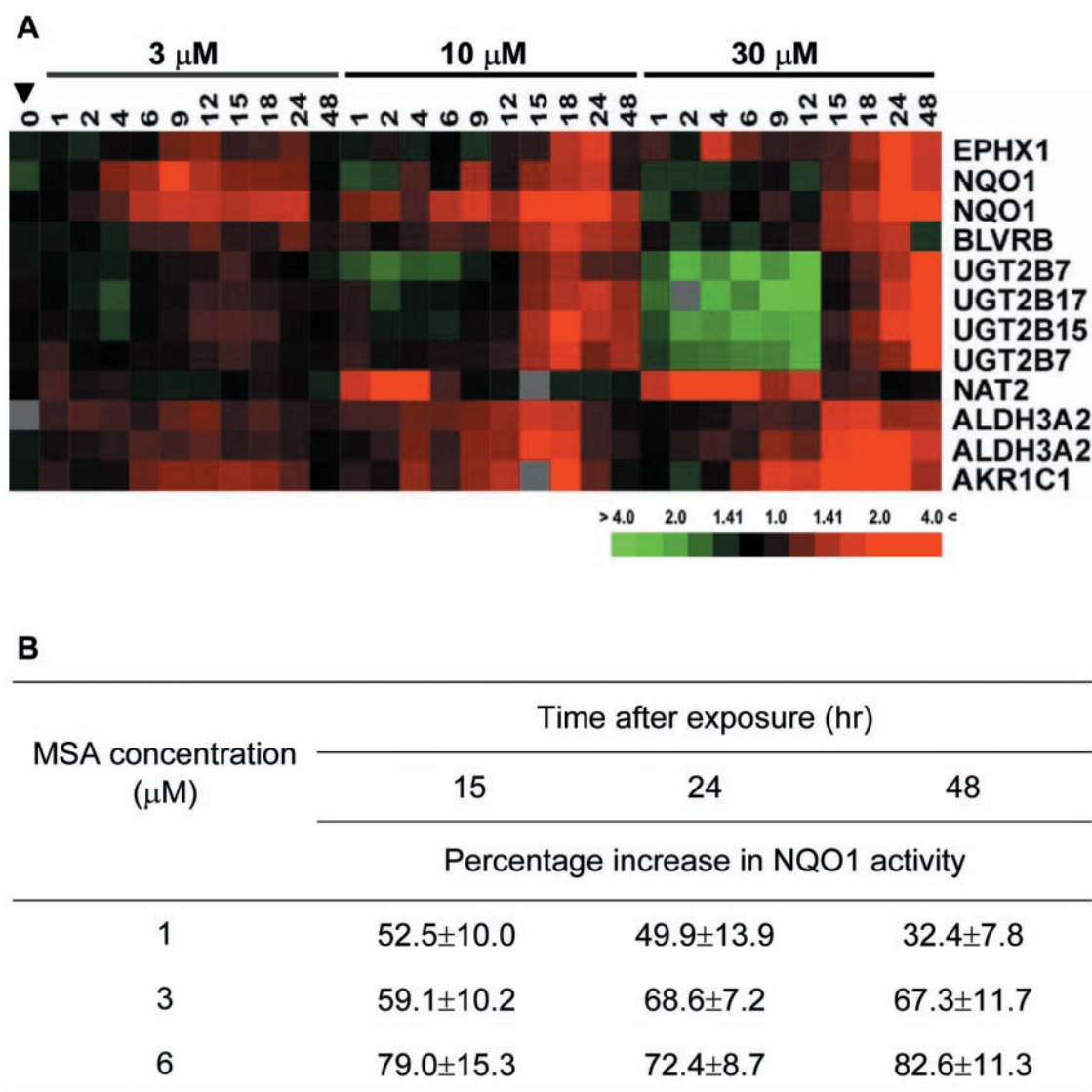


Figure 8. MSA induces expression of several phase 2 enzymes. Genes that occur more than once are represented by multiple clones on arrays. (A) Transcript levels of phase 2 enzymes after treatment with 3, 10, and 30 μM MSA. (B) Percentage increase of NQO1 enzymatic activity after treatment with 1, 3, and 6 μM MSA compared with untreated cells. Results shown represent the average of triplicate experiments.

gate marker of global phase 2 enzyme activity, were induced by as little as 3 μM MSA. At higher concentrations, several other phase 2 enzymes were induced coordinately with NQO1. We tested whether MSA also increases the enzymatic activity of NQO1 in LNCaP cells by a colorimetric assay involving the mendione-coupled reduction of tetrazolium dye (Brooks *et al.*, 2001b). Treated and control LNCaP cells were harvested at 15, 24, or 48 h after exposed to 1, 3, or 6 μM MSA. The NQO1 activity in each sample was normalized to the total protein of that sample, and the percentage of increase of NQO1 activity compared with control is shown in Figure 8B. NQO1 activity was induced similarly by all three concentrations of MSA and increased over time. Therefore, the increases in NQO1 transcript levels observed in the microarray experiments correlated well with induction of NQO1 enzymatic activity.

DISCUSSION

MSA induces striking dose- and time-dependent changes in gene expression in LNCaP cells, suggesting that selenium acts by diverse mechanisms as a putative prostate cancer preventive agent. MSA decreases proliferation of LNCaP cells, possibly by causing cells to exit the cell cycle, alters the expression of many genes in the androgen axis, including AR and many androgen-responsive genes, and induces expression of phase 2 detoxification enzymes, an effect that could be particularly relevant to human prostate cancer chemoprevention. Our findings support the hypothesis that monomethylated selenium may be responsible, at least in part, for the potential anticancer activity of selenium supplements.

Several reports using a variety of model systems have shown that selenium inhibits cell proliferation, and this

inhibition is thought to underlie selenium chemoprevention (Ip *et al.*, 2000a; Combs, 2001; Ganther, 2001; Lu, 2001). Decreased proliferation has been attributed to cell cycle arrest, although in prostate cancer cell lines no consistent pattern of arrest has been observed. After treatment with sodium selenite or selenomethionine, growth arrest has been reported in the G1 and G2/M phases of the cell cycle, depending on the prostate cancer cell line in which these compounds were tested (Redman *et al.*, 1998; Menter *et al.*, 2000; Venkateswaran *et al.*, 2002; Bhamre *et al.*, 2003). This lack of consistency may be due to innate differences between the cell lines or to differences in metabolism of the forms of selenium used in these studies. Based on compelling evidence that methylselenol is largely responsible for the chemopreventive activities of selenium compounds, we used MSA in our studies because it can be converted directly into methylselenol in vitro (Ip *et al.*, 2000b). MSA produced a dose-dependent inhibition of cell growth of LNCaP with an accumulation of cells in G0/G1 phase. Similar inhibition of proliferation and accumulation of cells in G0/G1 has been observed in breast cancer and endothelial cells treated with MSA (Sinha *et al.*, 2001; Wang *et al.*, 2001; Dong *et al.*, 2002).

We noted that a striking decrease in expression of many cell cycle-regulated genes from all phases of the cell cycle accompanied growth inhibition in LNCaP cells. Microarray analysis has been used in mammary cancer cells and PC-3 prostate cancer cells, and down-regulation of cell cycle-regulated genes has been observed along with increased expression of CDK inhibitors (Dong *et al.*, 2002, 2003). In these reports, decreased proliferation had been attributed to cell cycle arrest due to modulation of key regulators of the cell cycle, many of which are seen in our data set. Comparison of our data set to genes whose expression varies periodically as HeLa cells pass through the cell cycle provides a broader view of the effects of MSA on the cell cycle. The coordinate, decreased expression of genes involved in all phases of the cell cycle coupled with the increased expression of CDK-inhibitors (CDKN1A, CDKN2D, and CDKN1C) suggest MSA causes LNCaP cells to exit the cell cycle, rather than inducing an arrest at a specific phase in the cell cycle. Whether this is the primary mechanism by which selenium compounds inhibit cell growth awaits further study. Certainly, assessment of the effects of other forms of selenium on the expression of cell cycle genes in prostate cells could provide additional information on the means by which selenium compounds inhibit prostate cancer growth. Ultimately, it will be necessary to evaluate the effects of selenium on prostate cancer growth in vivo, and the cell cycle-regulated genes identified in this and other studies could serve as biomarkers of response.

Perhaps the most striking observation from our microarray experiments is that MSA produced changes in transcript levels of AR and AR-regulated genes. Androgens are critical to prostate carcinogenesis, and androgen deprivation therapy is a mainstay of prostate cancer treatment. MSA suppresses the expression of AR at both mRNA and protein levels, decreases transcript levels of PSA, and decreases PSA protein excretion into the media. A small set of well-characterized androgen-regulated genes, including those with androgen response regulatory elements, show expression changes that are reciprocal to those induced by androgen. Comparison of the MSA data set with a large data set of genes modulated in response to androgens shows that many, but not all, androgen-regulated genes show expression changes opposite to what is seen after treatment with androgens. Some genes were regulated similarly in the two data sets, suggesting that MSA has mixed effects on the

transcription of AR-regulated genes. It is possible that genes that are regulated similarly by MSA and androgens are not direct targets of androgen signaling pathways. For instance, androgen treatment of LNCaP cells is known to produce cellular stress by inducing an oxidative burst, and induction of stress response genes has been observed with expression profiling after androgen treatment (Xu *et al.*, 2001; DePrimo *et al.*, 2002). Therefore, the transcripts regulated similarly by androgens and MSA (DNAJB9, ATF3, and VEGF) might reflect cellular stress or other pathways that have been activated secondarily.

Effects of selenium on AR and AR-regulated genes in prostate cancer cell lines have not been observed with other selenium compounds; in fact, two reports have shown that selenomethionine does not have an effect on AR function or PSA secretion in LNCaP cells (Zhang *et al.*, 2002; Bhamre *et al.*, 2003). One possible explanation for the lack of effect of selenomethionine on androgen-regulated genes is its poor conversion to methylselenol in vitro. Intriguingly, men supplemented with selenized yeast do show small but significant decreases in their serum PSA levels compared with control subjects, suggesting the possibility that selenium compounds can affect AR-regulated genes in vivo where they can be metabolized to methylselenol (El-Bayoumy *et al.*, 2002). In addition, effects of MSA on AR-regulated genes in PC-3 cells were not observed by Dong *et al.* (2002, 2003), suggesting that MSA may affect transcription of AR-regulated genes through AR.

It is tempting to speculate that MSA blocks proliferation in prostate cells through its effects on AR and AR-regulated genes. Consistent with our findings, Venkateswaran *et al.* (200) observed that selenomethionine did not affect the growth of wild-type (AR-null) PC-3 prostate cancer cell lines, but did inhibit growth of PC-3 cells stably expressing AR. However, three other groups have observed growth inhibition by selenium compounds in prostate cancer cell lines that do not express AR (Redman *et al.*, 1998; Menter *et al.*, 2000; Dong *et al.*, 2003). Additional work will be necessary to understand the role of MSA on androgen signaling pathways and cell growth.

Our studies suggest that enhancement of detoxification is another mechanism that underlies the chemopreventive effects of MSA. MSA up-regulates mRNA levels of several phase 2 enzymes, including EPHX1, NQO1, NAT2, and members of the UGTB family, as well as the enzymatic activity of NQO1. We have observed similar induction of NQO1 enzymatic activity in LNCaP cells treated with sodium selenite and selenium dioxide (Brooks *et al.*, 2002), demonstrating that several forms of selenium are capable of inducing phase 2 enzymatic activity in prostate cells. Induction of phase 2 enzymatic activity has been proposed as a promising avenue of prostate cancer prevention after the discovery that virtually all human prostate cancers and precursor lesions (PIN) lose expression of the phase 2 enzyme glutathione S-transferase π (GSTP1) (DePrimo *et al.*, 2001; Nelson *et al.*, 2001). Global induction of phase 2 enzymes by selenium compounds might compensate for the loss of GSTP1 expression that occurs early in prostate carcinogenesis thereby and protect vulnerable prostatic epithelial cells against genome damage.

In summary, we have characterized the global transcriptional response program of LNCaP to MSA. The expression changes we observed imply that MSA exerts its anticancer activity through diverse mechanisms, including inhibition of cell proliferation, modulation of the expression of AR and its regulated genes, and induction of enzymes involved in carcinogen detoxification. Therefore, this data set provides a potential resource for understanding the modes of action of

MSA and serves as a source for candidate biomarkers of selenium's effects that could be measured *in vivo*. Discovery of such markers could help in the design and interpretation of selenium intervention trials currently in progress.

ACKNOWLEDGMENTS

We thank Dr. Zijie Sun for generously providing LNCaP cells, Dr. John Higgins for critical review of this manuscript, the Stanford Functional Genomics Facility for production of the high-quality microarrays used in this study, and the Stanford Microarray Database group for support on data storage and analysis. This work was supported by the Department of Defense (DAMD17-98-1-8555), the Doris Duke Foundation (T98064) and the Oxnard Foundation to J.D.B. M.L.W. is supported by a National Research Service Award Postdoctoral Fellowship from the National Human Genome Research Institute (HG00220) and by a grant from the Scleroderma Research Foundation.

REFERENCES

Andreadou, I., Menge, W.M., Commandeur, J.N., Worthington, E.A., and Vermeulen, N.P. (1996). Synthesis of novel Se-substituted selenocysteine derivatives as potential kidney selective prodrugs of biologically active selenol compounds: evaluation of kinetics of beta-elimination reactions in rat renal cytosol. *J. Med. Chem.* 39, 2040–2046.

Bhamre, S., Whitin, J.C., and Cohen, H.J. (2003). Selenomethionine does not affect PSA secretion independent of its effect on LNCaP cell growth. *Prostate* 54, 315–321.

Blader, I.J., Manger, I.D., and Boothroyd, J.C. (2001). Microarray analysis reveals previously unknown changes in *Toxoplasma gondii*-infected human cells. *J. Biol. Chem.* 276, 24223–24231.

Brooks, J.D., Goldberg, M.F., Nelson, L.A., Wu, D., and Nelson, W.G. (2002). Identification of potential prostate cancer preventive agents through induction of quinone reductase *in vitro*. *Cancer Epidemiol. Biomarkers Prev.* 11, 868–875.

Brooks, J.D., Metter, E.J., Chan, D.W., Sokoll, L.J., Landis, P., Nelson, W.G., Muller, D., Andres, R., and Carter, H.B. (2001a). Plasma selenium level before diagnosis and the risk of prostate cancer development. *J. Urol.* 166, 2034–2038.

Brooks, J.D., Paton, V.G., and Vidanes, G. (2001b). Potent induction of phase 2 enzymes in human prostate cells by sulforaphane. *Cancer Epidemiol. Biomarkers Prev.* 10, 949–954.

Clark, L.C., *et al.* (1996). Effects of selenium supplementation for cancer prevention in patients with carcinoma of the skin. A randomized controlled trial. Nutritional Prevention of Cancer Study Group. *J. Am. Med. Assoc.* 276, 1957–1963.

Clark, L.C., *et al.* (1998). Decreased incidence of prostate cancer with selenium supplementation: results of a double-blind cancer prevention trial. *Br. J. Urol.* 81, 730–734.

Combs, G.F., Jr. (2001). Considering the mechanisms of cancer prevention by selenium. *Adv. Exp. Med. Biol.* 492, 107–117.

Davis, C.D., Zeng, H., and Finley, J.W. (2002). Selenium-enriched broccoli decreases intestinal tumorigenesis in multiple intestinal neoplasia mice. *J. Nutr.* 132, 307–309.

DePrimo, S.E., Diehn, M., Nelson, J.B., Reiter, R.E., Matese, J., Fero, M., Tibshirani, R., Brown, P.O., and Brooks, J.D. (2002). Transcriptional programs activated by exposure of human prostate cancer cells to androgen. *Genome Biol.* 3, RESEARCH0032.

DePrimo, S.E., Shinghal, R., Vidanes, G., and Brooks, J.D. (2001). Prevention of prostate cancer. *Hematol. Oncol. Clin. North Am.* 15, 445–457.

Dong, Y., Ganther, H.E., Stewart, C., and Ip, C. (2002). Identification of molecular targets associated with selenium-induced growth inhibition in human breast cells using cDNA microarrays. *Cancer Res.* 62, 708–714.

Dong, Y., Zhang, H., Hawthorn, L., Ganther, H.E., and Ip, C. (2003). Delineation of the molecular basis for selenium-induced growth arrest in human prostate cancer cells by oligonucleotide array. *Cancer Res.* 63, 52–59.

Duffield-Lillico, A.J., Reid, M.E., Turnbull, B.W., Combs, G.F., Jr., Slate, E.H., Fischbach, L.A., Marshall, J.R., and Clark, L.C. (2002). Baseline characteristics and the effect of selenium supplementation on cancer incidence in a randomized clinical trial: a summary report of the Nutritional Prevention of Cancer Trial. *Cancer Epidemiol. Biomarkers Prev.* 11, 630–639.

Eisen, M.B., Spellman, P.T., Brown, P.O., and Botstein, D. (1998). Cluster analysis and display of genome-wide expression patterns. *Proc. Natl. Acad. Sci. USA* 95, 14863–14868.

el-Bayoumy, K. (1994). Evaluation of chemopreventive agents against breast cancer and proposed strategies for future clinical intervention trials. *Carcinogenesis* 15, 2395–2420.

El-Bayoumy, K. (2001). The protective role of selenium on genetic damage and on cancer. *Mutat. Res.* 475, 123–139.

El-Bayoumy, K., Richie, J.P., Jr., Boyiri, T., Komninou, D., Prokopczyk, B., Trushin, N., Kleinman, W., Cox, J., Pittman, B., and Colosimo, S. (2002). Influence of selenium-enriched yeast supplementation on biomarkers of oxidative damage and hormone status in healthy adult males: a clinical pilot study. *Cancer Epidemiol. Biomarkers Prev.* 11, 1459–1465.

Fleming, J., Ghose, A., and Harrison, P.R. (2001). Molecular mechanisms of cancer prevention by selenium compounds. *Nutr. Cancer* 40, 42–49.

Ganther, H.E. (2001). Selenium metabolism and mechanisms of cancer prevention. *Adv. Exp. Med. Biol.* 492, 119–130.

Ganther, H.E., and Lawrence, J.R. (1997). Chemical transformations of selenium in living organisms. Improved forms of selenium for cancer prevention. *Tetrahedron* 53, 12299–12310.

Gitig, D.M., and Koff, A. (2000). Cdk pathway: cyclin-dependent kinases and cyclin-dependent kinase inhibitors. *Methods Mol. Biol.* 142, 109–123.

Groszer, M., Erickson, R., Scripture-Adams, D.D., Lesche, R., Trumpp, A., Zack, J.A., Kornblum, H.L., Liu, X., and Wu, H. (2001). Negative regulation of neural stem/progenitor cell proliferation by the Pten tumor suppressor gene *in vivo*. *Science* 294, 2116–2118.

Helzlsouer, K.J., Huang, H.Y., Alberg, A.J., Hoffman, S., Burke, A., Norkus, E.P., Morris, J.S., and Comstock, G.W. (2000). Association between alpha-tocopherol, gamma-tocopherol, selenium, and subsequent prostate cancer. *J. Natl. Cancer Inst.* 92, 2018–2023.

Hoque, A., *et al.* (2001). Molecular epidemiologic studies within the Selenium and Vitamin E Cancer Prevention Trial (SELECT). *Cancer Causes Control* 12, 627–633.

Ip, C. (1998). Lessons from basic research in selenium and cancer prevention. *J. Nutr.* 128, 1845–1854.

Ip, C., Hayes, C., Budnick, R.M., and Ganther, H.E. (1991). Chemical form of selenium, critical metabolites, and cancer prevention. *Cancer Res.* 51, 595–600.

Ip, C., Thompson, H.J., and Ganther, H.E. (2000a). Selenium modulation of cell proliferation and cell cycle biomarkers in normal and premalignant cells of the rat mammary gland. *Cancer Epidemiol. Biomarkers Prev.* 9, 49–54.

Ip, C., Thompson, H.J., Zhu, Z., and Ganther, H.E. (2000b). *In vitro* and *in vivo* studies of methylseleninic acid: evidence that a monomethylated selenium metabolite is critical for cancer chemoprevention. *Cancer Res.* 60, 2882–2886.

Ip, C., and White, G. (1987). Mammary cancer chemoprevention by inorganic and organic selenium: single agent treatment or in combination with vitamin E and their effects on *in vitro* immune functions. *Carcinogenesis* 8, 1763–1766.

Jiang, C., Wang, Z., Ganther, H., and Lu, J. (2001). Caspases as key executors of methyl selenium-induced apoptosis (anoikis) of DU-145 prostate cancer cells. *Cancer Res.* 61, 3062–3070.

Jones, J.O., and Arvin, A.M. (2003). Microarray analysis of host cell gene transcription in response to Varicella-Zoster virus infection of human t cells and fibroblasts *in vitro* and scidhu skin xenografts *in vivo*. *J. Virol.* 77, 1268–1280.

Kim, Y.S., and Milner, J. (2001). Molecular targets for selenium in cancer prevention. *Nutr. Cancer* 40, 50–54.

Klein, E.A., Thompson, I.M., Lippman, S.M., Goodman, P.J., Albanes, D., Taylor, P.R., and Coltman, C. (2001). SELECT: the next prostate cancer prevention trial. Selenium and Vitamin E Cancer Prevention Trial. *J. Urol.* 166, 1311–1315.

Lu, J. (2001). Apoptosis and angiogenesis in cancer prevention by selenium. *Adv. Exp. Med. Biol.* 492, 131–145.

Lu, J., and Jiang, C. (2001). Antiangiogenic activity of selenium in cancer chemoprevention: metabolite-specific effects. *Nutr. Cancer* 40, 64–73.

Lyons, A.B. (2000). Analysing cell division *in vivo* and *in vitro* using flow cytometric measurement of CFSE dye dilution. *J. Immunol. Methods* 243, 147–154.

Medina, D., Thompson, H., Ganther, H., and Ip, C. (2001). Se-methylselenocysteine: a new compound for chemoprevention of breast cancer. *Nutr. Cancer* 40, 12–17.

Menter, D.G., Sabichi, A.L., and Lippman, S.M. (2000). Selenium effects on prostate cell growth. *Cancer Epidemiol. Biomarkers Prev.* 9, 1171–1182.

Nelson, P.S., Clegg, N., Arnold, H., Ferguson, C., Bonham, M., White, J., Hood, L., and Lin, B. (2002). The program of androgen-responsive genes in neoplastic prostate epithelium. *Proc. Natl. Acad. Sci. USA* 99, 11890–11895.

- Nelson, W.G., De Marzo, A.M., Dewese, T.L., Lin, X., Brooks, J.D., Putzi, M.J., Nelson, C.P., Groopman, J.D., and Kensler, T.W. (2001). Preneoplastic prostate lesions: an opportunity for prostate cancer prevention. *Ann. N.Y. Acad. Sci.* 952, 135–144.
- Nomura, A.M., Lee, J., Stemmermann, G.N., and Combs, G.F., Jr. (2000). Serum selenium and subsequent risk of prostate cancer. *Cancer Epidemiol. Biomarkers Prev.* 9, 883–887.
- Rao, C.V., Wang, C.Q., Simi, B., Rodriguez, J.G., Cooma, I., El-Bayoumy, K., and Reddy, B.S. (2001). Chemoprevention of colon cancer by a glutathione conjugate of 1,4-phenylenebis(methylene)selenocyanate, a novel organoselenium compound with low toxicity. *Cancer Res.* 61, 3647–3652.
- Reddy, B.S., Upadhyaya, P., Simi, B., and Rao, C.V. (1994). Evaluation of organoselenium compounds for potential chemopreventive properties in colon carcinogenesis. *Anticancer Res.* 14, 2509–2514.
- Redman, C., Scott, J.A., Baines, A.T., Basye, J.L., Clark, L.C., Calley, C., Roe, D., Payne, C.M., and Nelson, M.A. (1998). Inhibitory effect of selenomethionine on the growth of three selected human tumor cell lines. *Cancer Lett.* 125, 103–110.
- Sherlock, G., *et al.* (2001). The Stanford microarray database. *Nucleic Acids Res.* 29, 152–155.
- Sherr, C.J., and Roberts, J.M. (1999). CDK inhibitors: positive and negative regulators of G1-phase progression. *Genes Dev.* 13, 1501–1512.
- Sinha, R., Unni, E., Ganther, H.E., and Medina, D. (2001). Methylseleninic acid, a potent growth inhibitor of synchronized mouse mammary epithelial tumor cells in vitro. *Biochem. Pharmacol.* 61, 311–317.
- Venkateswaran, V., Klotz, L.H., and Fleshner, N.E. (2002). Selenium modulation of cell proliferation and cell cycle biomarkers in human prostate carcinoma cell lines. *Cancer Res.* 62, 2540–2545.
- Wang, Z., Jiang, C., Ganther, H., and Lu, J. (2001). Antimitogenic and proapoptotic activities of methylseleninic acid in vascular endothelial cells and associated effects on PI3K-AKT, ERK, JNK and p38 MAPK signaling. *Cancer Res.* 61, 7171–7178.
- Whitfield, M.L., *et al.* (2002). Identification of genes periodically expressed in the human cell cycle and their expression in tumors. *Mol. Biol. Cell* 13, 1977–2000.
- Willett, W.C., Polk, B.F., Morris, J.S., Stampfer, M.J., Pressel, S., Rosner, B., Taylor, J.O., Schneider, K., and Hames, C.G. (1983). Prediagnostic serum selenium and risk of cancer. *Lancet* 2, 130–134.
- Williams, E.D., and Brooks, J.D. (2001). New molecular approaches for identifying novel targets, mechanisms, and biomarkers for prostate cancer chemopreventive agents. *Urology* 57, 100–102.
- Xu, L.L., Su, Y.P., Labiche, R., Segawa, T., Shanmugam, N., McLeod, D.G., Moul, J.W., and Srivastava, S. (2001). Quantitative expression profile of androgen-regulated genes in prostate cancer cells and identification of prostate-specific genes. *Int. J. Cancer* 92, 322–328.
- Yoshizawa, K., Willett, W.C., Morris, S.J., Stampfer, M.J., Spiegelman, D., Rimm, E.B., and Giovannucci, E. (1998). Study of prediagnostic selenium level in toenails and the risk of advanced prostate cancer. *J. Natl. Cancer Inst.* 90, 1219–1224.
- Youn, B.W., Fiala, E.S., and Sohn, O.S. (2001). Mechanisms of organoselenium compounds in chemoprevention: effects on transcription factor-DNA binding. *Nutr. Cancer* 40, 28–33.
- Zhang, Y., Ni, J., Messing, E.M., Chang, E., Yang, C.R., and Yeh, S. (2002). Vitamin E succinate inhibits the function of androgen receptor and the expression of prostate-specific antigen in prostate cancer cells. *Proc. Natl. Acad. Sci. USA* 99, 7408–7413.
- Zhao, H., Hastie, T., Whitfield, M.L., Borresen-Dale, A.L., and Jeffrey, S.S. (2002). Optimization and evaluation of T7 based RNA linear amplification protocols for cDNA microarray analysis. *BMC Genomics* 3, 31
- Zhu, Z., Jiang, W., Ganther, H.E., and Thompson, H.J. (2002). Mechanisms of cell cycle arrest by methylseleninic acid. *Cancer Res.* 62, 156–164.

Molecular Targets of Doxazosin in Human Prostatic Stromal Cells

Hongjuan Zhao, Frank Lai, Larisa Nonn, James D. Brooks,
and Donna M. Peehl*

Department of Urology, Stanford University School of Medicine, Stanford, California

BACKGROUND. We used cDNA microarray analysis to obtain insights into the mechanisms of action of doxazosin, an α_1 -adrenergic receptor antagonist used to treat benign prostatic hyperplasia (BPH).

METHODS. Hierarchical clustering analysis and significance analysis of microarray (SAM) were performed to identify genes differentially expressed between untreated stromal cells cultured from normal tissue and BPH, and changes in gene expression induced by doxazosin. Transcript levels of selected genes were validated by real-time reverse-transcription polymerase chain reaction (RT-PCR).

RESULTS. Hierarchical clustering analyses separated untreated normal and BPH cells. Sixty-seven genes whose expression varied at least twofold after doxazosin treatment in both normal and BPH cells were identified, as were 93 genes differentially regulated in normal versus BPH cells. Molecular targets consistent with tumor necrosis factor (TNF)- α -related activity were identified.

CONCLUSIONS. Normal versus BPH stromal cells differ in global gene transcription. Doxazosin induced gene expression changes relevant to proliferation/apoptosis, immune defense, cell–cell signaling/signal transduction, and transcriptional regulation. *Prostate* 62: 400–410, 2005. © 2004 Wiley-Liss, Inc.

KEY WORDS: adrenergic receptor; benign prostatic hyperplasia; transforming growth factor- β ; tumor necrosis factor- α

INTRODUCTION

Benign prostatic hyperplasia (BPH) is a common disease of older men, causing urinary obstructive symptoms that require clinical intervention in more than 35% of men age 50 or older in the United States each year [1]. Antagonists of α_1 -adrenergic receptors including doxazosin, terazosin, tamsulosin, and afluzosin are used to alleviate the symptoms of BPH [2], since blockade of adrenergic receptors in prostatic smooth muscle relaxes muscle tone, relieving constrictive pressure of the enlarged prostate on the urethra. Doxazosin, in particular, has drawn a great deal of interest from both clinicians and basic research scientists because it is a first-line antihypertensive agent in addition to its use in treating BPH [2].

Studies on the mechanisms of actions of doxazosin and terazosin have revealed unanticipated adrenergic receptor-independent activities that may be relevant to their long-term effects in patients with BPH [3]. Specifically, increased rates of apoptosis have been observed

in both the epithelium and stroma of BPH tissues in men treated with doxazosin and terazosin. Induction of apoptosis by doxazosin or terazosin was also shown in cultured prostatic stromal cells and in prostate cancer cell lines. Doxazosin's apoptotic activity is not specific to prostate cells but extends to skin fibroblasts and non-prostatic cancer cell lines as well. However, some cells, such as normal prostatic epithelial cells and bladder and colon cell lines, are resistant to doxazosin-induced apoptosis for unknown reasons. Apoptosis occurs in

Grant sponsor: Pfizer, Inc. (International Cardura Competitive Award); Grant sponsor: United States Army MPMC Prostate Cancer Research Program (Postdoctoral Traineeship Award); Grant number: W81XWH-04-1-0080.

*Correspondence to: Donna M. Peehl, PhD, Department of Urology, Stanford Medical Center, Stanford, CA 94305-5118.

E-mail: dpeehl@stanford.edu

Received 29 April 2004; Accepted 7 July 2004

DOI 10.1002/pros.20161

Published online 17 September 2004 in Wiley InterScience

(www.interscience.wiley.com).

cells lacking α_1 -adrenoceptors and/or in the presence of excess agonists, demonstrating that the apoptotic activity of doxazosin and terazosin is not mediated by antagonism of adrenoceptors. These effects are limited to the quinazoline-derived α_1 -antagonists doxazosin and terazosin and do not extend to the sulfonamide-based antagonist, tamulosin.

The apoptotic potential of doxazosin and terazosin adds a new dimension not only to use of these drugs in treating BPH but also with regard to potential chemotherapeutic or chemopreventive activity against prostate cancer. However, the mechanism by which these drugs induce apoptosis is not clear. Some evidence suggests that apoptosis may result from activation of the transforming growth factor (TGF)- β signal transduction pathway [3]. To gain new insights into the mechanisms of action of these drugs, we identified molecular targets of doxazosin on a genome-wide scale using cDNA microarrays containing 42,941 elements. Transcript levels in primary cultures of prostatic stromal cells derived from normal transition zone and BPH tissues with or without doxazosin treatment were compared. Gene expression changes in response to doxazosin were determined by hierarchical clustering and significance analysis of microarray (SAM) analysis, and further validated by quantitative real-time reverse transcription-polymerase chain reaction (RT-PCR). The involvement of TGF- β in doxazosin-induced apoptosis was assessed in the microarray data and by cell-based assays. Overall, our results implicate a tumor necrosis factor (TNF)- α -related signaling pathway associated with an increase in reactive oxygen species (ROS) and do not support the involvement of a TGF- β pathway in doxazosin-induced apoptosis in prostatic stromal cells.

MATERIALS AND METHODS

Isolation, Culture, and Doxazosin Treatment of Prostatic Stromal Cells

Primary cultures of human prostatic stromal cells were established from histologically confirmed BPH tissue of a 65-year-old man and from normal (without BPH) transition zone tissue of a 42-year-old man according to previously described methods [4]. The presence of contaminating epithelial cells was ruled out by the absence of staining with antibodies against epithelial keratins 5 and 18 (Enzo Life Sciences, Inc., Farmingdale, NY). These cultures (designated F-BPH-32 and F-TZ-55, respectively) were serially passaged in MCDB 105 (Sigma-Aldrich, St. Louis, MO) supplemented with 10% fetal bovine serum (FBS) and 100 μ g/ml of gentamycin. At passages 10 and 11 (F-BPH-32) and 16 (F-TZ-55), semi-confluent cells were fed fresh medium 2 days prior to the addition of 50 μ M of doxazosin (Pfizer, Inc., New York, NY) or diluent [0.1% dimethylsulfoxide

(DMSO)] at t_0 in duplicate experiments. Total RNA was isolated using an RNeasy kit (Qiagen, Chatsworth, CA) at 2, 8 and, in one experiment, 24 hr. This dose of doxazosin was selected because it has been shown to cause apoptosis in cultured human prostatic stromal cells [3].

cDNA Microarray Hybridizations

Fluorescently-labeled cDNA probes were prepared from 50 to 70 μ g total RNA isolated from doxazosin-treated or diluent-treated cells (Cy5-labeled) and Universal Human Reference RNA (Stratagene, La Jolla, CA) (Cy3-labeled) by reverse transcription using an Oligo dT primer 5'-TTTTTTTTTTTTTTTT-3' (Qiagen) as described previously [5]. Labeled probes from doxazosin-treated and control cells for each time point were mixed and hybridized overnight at 65°C to spotted cDNA microarrays with 42,941 elements (Stanford Functional Genomics Facility). Microarray slides were then washed to remove unbound probe and scanned with a GenePix 4000B scanner (Axon Instruments, Inc., Union City, CA).

Data Processing and Analysis

The acquired fluorescence intensities for each fluorophore were analyzed with GenePix Pro 3.0 software (Axon Instruments, Inc.). Spots of poor quality were removed from further analysis by visual inspection. Data files containing fluorescence ratios were entered into the Stanford Microarray Database (SMD) where biological data were associated with fluorescence ratios and genes were selected for further analysis [6]. Hierarchical clustering was performed by first retrieving only spots with a signal intensity >150% above background in both Cy5- and Cy3-channels in at least 80% of the microarray experiments from SMD. We selected clones whose expression levels varied at least twofold in at least two of the samples from the mean abundance across all samples included in a specific analysis as indicated. Common genes among different data sets were identified using Microsoft Excel. The genes and arrays in the resulting data tables were ordered by their patterns of gene expression using hierarchical clustering analysis [7], and visualized using Treeview software (<http://rana.lbl.gov/EisenSoftware.htm>).

Genes with potentially significant changes in expression in response to doxazosin were identified using the SAM procedure [8], which computes a two-sample T-statistic (e.g., for doxazosin-treated vs. untreated cells) for the normalized log ratios of gene expression levels for each gene. The procedure thresholds the T-statistics to provide a 'significant' gene list and provides an estimate of the false-discovery rate (the percentage of genes identified by chance alone) from

randomly permuted data. We used a selection threshold that gives the lowest false discovery rate and identifies the highest number of significant genes.

Quantitative Real-Time RT-PCR

Total RNA from untreated and treated cells was reverse transcribed as described above. cDNA product was then mixed with iQTM SYBR[®] Green Supermix (Bio-Rad, Hercules, CA) and primers of choice in the subsequent PCR reaction using an iCycler iQ real-time PCR Detection System (Bio-Rad) according to manufacture's instructions. Each reaction was done in triplicate to minimize the experimental variations (standard deviation was calculated for each reaction). Transcript levels of GAPDH were assayed simultaneously with each of the following ten genes as an internal control to normalize their transcript levels in treated and untreated cells. When compared to microarray data, transcript levels of multiple clones representing the same gene were averaged and standard deviation was calculated. The primer sequences used were: *IL6* (5'ATGCAATAACCACCCCTGAC3' and 5'TAAAGCTGCGCAGAATGAGA3'), *EGR1* (5'ACCGCAGAGTCTTTTCCTGA3' and 5'AGCCAAGACGATGAAGCAGT3'), *TNFAIP3* (5' AACTGGCAAGGGATGATGTC3' and 5'AGCCAAGACGATGAAGCAGT3'), *JUNB* (5'GGACGATCTGCACAAGATGA3' and 5'GTTGGTGTAACGGGAGGTG3'), *TNXIP* (5'CCTCTGGGACATCCTTCAA3' and 5'GGGGTATTGACATCCACCAG3'), *INSIG1* (5'CATTAACCACGCCATCCTCAA3' and 5'CTGGAACGATCAAATGTCCA3'), *GADD45B* (5' GTGTAXGAGTXGGXXAAGTT3' and 5'TGTCACAGCAGAAGGACTGG3'), *CYP11B1* (5'CCAAGGACACTGTGGTTTT3' and 5'TCATCACTCTGCTGGTCAGG3'), *SFTPC* (5'CTCCACCATGAGCAGAAACA3' and 5'GGAGAAGGTGGCAGTGGTAA3'), *HMOX1* (5'TCTCTGGCTGGCTTCCTTA3' and 5'ATTGCCTGGATGTGCTTTTC3'), and *GAPDH* (5'CGACCACTTTGTCAAGCTCA3' and 5'GGGTCTTACTCCTTGGAGGC3').

Measurement of Mitochondrial Membrane Potential

Cells were inoculated at 10,000 per well into 96-well black-sided dishes containing MCDB 105 with 10% FBS and 100 µg/ml of gentamycin. The next day, reagents were added to triplicate wells. Reagents included doxazosin, TGF-β₁ (PeproTech, Inc., Rocky Hill, NJ), TNF-α (PeproTech, Inc.), pan-neutralizing antibody against TGF-β (R&D Systems, Minneapolis, MN) and non-immune mouse IgG (Sigma-Aldrich). At various time points, mitochondrial membrane potential was measured by using the mitochondrial specific cationic fluorescent dye (JC-1) (Molecular Probes, Eugene, OR)

that is sensitive to changes in membrane potential as described by Weitsman et al. [9]. Briefly, growth medium was replaced with JC-1-containing medium (5 µg/ml) and incubated at 37°C for 30 min. Wells were rinsed twice in medium without phenol red and then allowed to equilibrate in the medium for 30 min at 37°C. JC-1 fluorescence was analyzed at 540/590 nm for the red J-aggregate (−ΔΨ) and 490/540 for the green monomer (intact ΔΨ) using the SpetroMax Gemini XS Fluorescent Plate reader (Molecular Devices, Sunnyvale, CA). Mitochondrial membrane potential is represented by the ratio of 590/525 nm emission (+ΔΨ/−ΔΨ) and this ratio is independent of cell number, mitochondrial shape, size, and density.

Measurement of ROS by CM-H2DCFDA

Cells were inoculated at 10,000 per well into 96-well black-sided dishes containing MCDB 105 with 10% FBS and 100 µg/ml of gentamycin. The next day, cells were loaded with 36 µM CM-H2DCFDA (Molecular Probes) in medium for 30 min at 37°C. Wells were rinsed twice in fresh medium and then dosed with medium containing doxazosin or DMSO. After 6 hr, cells were analyzed at 460/525 nm using a SpetroMax Gemini XS Fluorescent Plate reader.

Measurement of TNF-α by ELISA

Cells were inoculated at 50,000 per well into 96-well plates containing MCDB 105 with 10% FBS and 100 µg/ml of gentamycin. Two days later, diluent or doxazosin was added without changing the medium. Conditioned media were collected at 24 and 48 hr and stored at −70°C after centrifuging to remove debris. Concentrations of TNF-α in the media were measured with a high sensitivity human TNF-α ELISA system (Amersham Biosciences, Piscataway, NJ).

RESULTS

Gene Expression in Untreated Normal Versus BPH Stromal Cells

A hierarchical clustering analysis of 1,111 named unique genes represented by 1,385 clones whose expression varied at least twofold from the overall mean abundance in at least two samples in untreated normal and BPH stromal cells is shown in Figure 1. In the dendrogram, normal stromal cells were separated completely from BPH stromal cells, demonstrating that prostate stromal cells from normal and BPH tissues can be clearly distinguished based on their distinct gene expression patterns. Within each group of samples, cells from the same passage clustered together, probably reflecting the effects of non-intrinsic factors such as culture conditions on the transcriptional program of

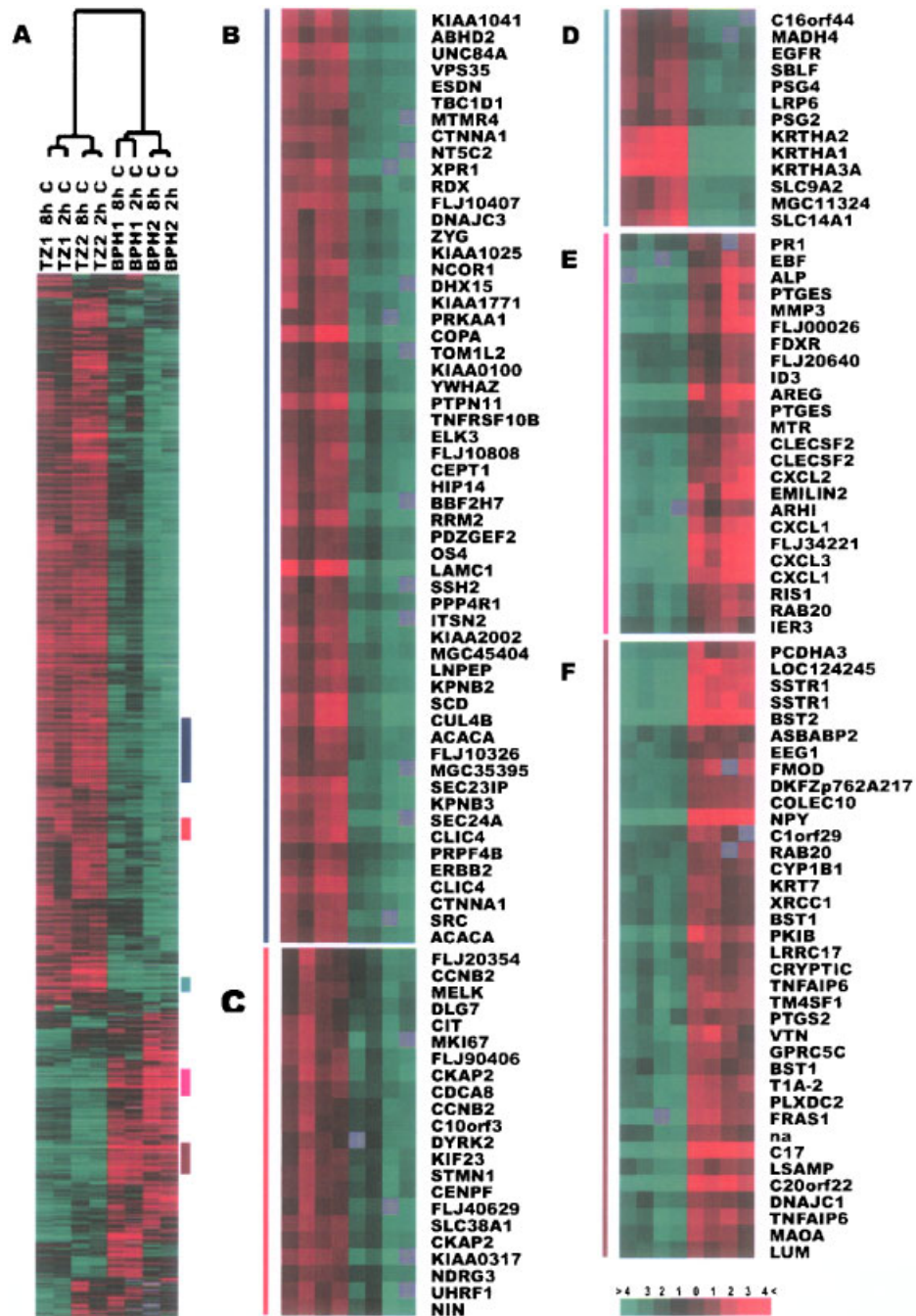


Fig. 1. Different gene expression patterns between untreated normal and benign prostatic hyperplasia (BPH) stromal cells shown by hierarchical clustering analysis. Genes that appear more than once are represented by multiple clones on arrays. Both genes (represented by rows) and samples (represented by columns) were clustered according to their similarities in expression patterns. For each cell type, BPH and normal transition zone (TZ), four samples from two different passages (1 vs. 2) grown for different lengths of time (8 hr sample was harvested 6 hr later after the 2 hr sample) were assayed, and the dendrogram of cluster shown on **top** of the overview image (**A**). The degree of color saturation corresponds to the ratio of gene expression shown at the **bottom** of the image. **B–F** are zoomed images of clusters of genes that are differentially expressed between the two cell types. (**B, F**) Clusters with genes involved in diverse biological processes; (**C**) cell-cycle-regulated gene enriched cluster; (**D**) hair keratin enriched cluster; (**E**) chemokine enriched cluster. [Color figure can be viewed in the online issue, which is available at www.interscience.wiley.com.]

the cells. Out of the 1,111 differentially expressed genes, 779 were overexpressed in normal stromal cells compared to BPH stromal cells, and 329 were under-expressed. The remaining three genes each represented by multiple clones could not be classified because different clones pointed to different expression trends (for full list of genes, see web supplement <http://www.stanford.edu/~hongjuan/Doxazosin/>). Some of the genes showed expression variations in almost all eight samples (Fig. 1B–F), while others were present only in a portion of the samples.

Although most of the clusters contained genes implicated in a variety of biological processes (Fig. 1B,F), some clusters were enriched with genes involved in a particular aspect of the life cycle of the cells. For example, when compared to a data set on cell-cycle-regulated genes generated by Whitfield et al. in HeLa cells [10], 13 genes (*FLJ20345*, *CCNB2*, *MELK*, *DLG7*, *CIT*, *MKI67*, *CKAP2*, *CDC48*, *C10orf3*, *KIF23*, *CENPF*, *FLJ40629*, *UHRF1*) that are cell-cycle-regulated were present in one cluster (Fig. 1C) which also contains two genes (*STMN1* and *NDRG3*) involved in cell-growth regulation. Interestingly, 12 of these 13 cell-cycle-regulated genes showed peak expression in G₂ or G₂/M, phases of the cell cycle, except for *UHRF1* in G₁/S phase. Three members of the hair keratins (*KRTHA1*, 2, and 3A), which are components of intermediate filaments, were strongly underexpressed in BPH cells compared to normal stromal cells (Fig. 1D), whereas three chemokines (*CXCL1*, 2, and 3), which are involved in a number of biological processes such as cell proliferation, immune response, and signal transduction, were overexpressed in BPH cells (Fig. 1E).

Gene Expression in Doxazosin-Treated Stromal Cells

Figure 2 shows a hierarchical clustering analysis of doxazosin-induced gene expression changes in normal and BPH prostatic stromal cells at 2 and 8 hr (and at 24 hr in one experiment with BPH cells). After eliminating the “intrinsic” differences in gene expression between normal and BPH cells (see above) by separately mean centering the gene expression of these two cell types, 332 clones representing 283 unique named genes were selected and grouped by the similarities of their expression patterns (for full list of genes, see web supplement <http://www.stanford.edu/~hongjuan/Doxazosin/>). Several features of doxazosin-induced gene expression are apparent from the cluster pattern. First, doxazosin induced gene expression changes in normal and BPH cells in a time-dependent manner. The magnitude of expression variations observed after 8 and 24 hr treatments was much larger than after 2 hr treatment. Second, doxazosin increased expression of

the vast majority of the responsive genes, and suppressed expression of only minimal number of genes (Fig. 2B). Third, genes involved in a particular biological process clustered together. For example, 20 clones representing 12 genes involved in cell proliferation and apoptosis were grouped together (Fig. 2C). Five transcription factors and four genes involved in immune responses also clustered together (Fig. 2D,E). Finally, expression of some genes was affected in only one cell type but not the other (Fig. 2F).

When SAM analysis was performed on the 332 clones, 250 representing 115 unique named genes were selected as significant differentially expressed with a false discovery rate of 0.1%. Out of the 115 genes, 67 genes with known functions whose expression after averaging duplicate experiments varied at least twofold in response to doxazosin after 8 hr of treatment are listed in Table I and grouped according to function in GO annotation. The majority of these (64 genes) were up-regulated, with only three genes down-regulated by doxazosin. Of the up-regulated genes, *TNFAIP3* and *INSIG1* were the most highly induced (greater than eightfold in both normal and BPH cells). Other highly up-regulated genes (greater than fivefold) in both normal and BPH cells included *GOS2*, *NR4A1*, *PTGS2*, *IL-6*, and *HMOX1*. The most highly down-regulated gene in both types of stromal cells was *TXNIP*. In addition, 30 genes showed expression variations greater than twofold (20 genes up-regulated and 10 genes down-regulated) in response to doxazosin in BPH cells but not in normal cells, and 63 genes vice versa (48 up-regulated and 15 down-regulated) (for full list of genes, see web supplement <http://www.stanford.edu/~hongjuan/Doxazosin/>).

Validation of Selected Genes by Quantitative Real-Time RT-PCR

To confirm the gene expression changes observed by microarray analysis, real-time RT-PCR was performed on ten selected genes. Their expression changes assessed by both methods after 8 hr treatment in duplicate samples from normal and BPH cells are listed in Table II. When the array data was paired with the RT-PCR data, only one of the 40 data pairs (*GADD45B* in BPH) showed small expression variations in different directions. In 29 out of the 40 data pairs (72.5%), expression change determined by RT-PCR differed from that by microarray by less than 50%, and seven data pairs (17.5%) differed between 50 and 100%. Only in 4 (10%) of the data pairs did gene expression changes observed by RT-PCR differ from that by microarray by more than 100%. These results suggest that the gene expression changes in response to doxazosin obtained using microarray are reliable.

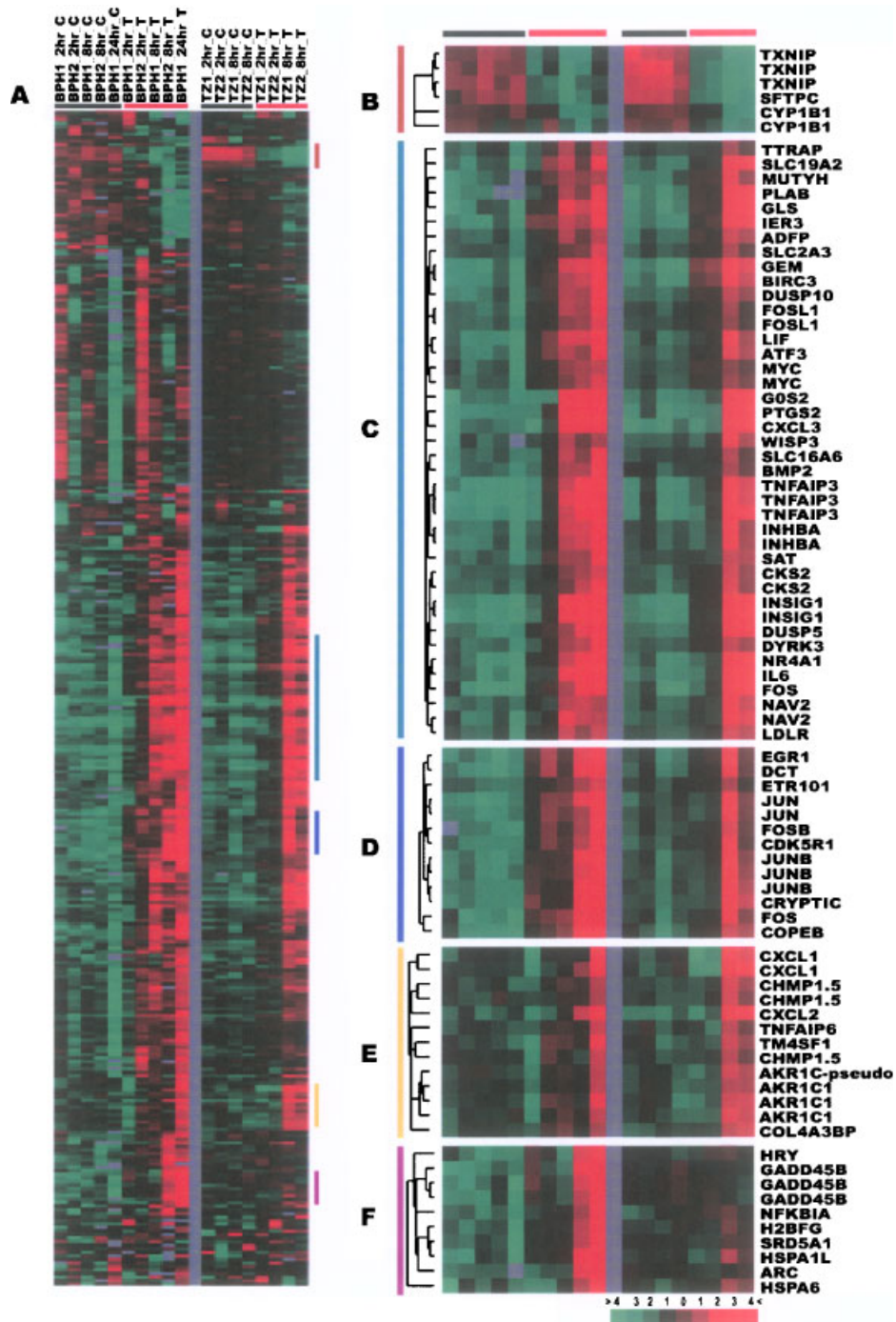


Fig. 2. Hierarchical clustering analysis of doxazosin-induced gene expression changes in prostatic stromal cells. Each column represents data from a single time point with or without doxazosin treatment, and each row represents expression levels for a single gene across the time course. The responses to doxazosin by stromal cells isolated from BPH and TZ were separated by a gray column. The data from each cell type were arranged such that the gene expression pattern of untreated cells (black bar) was shown to the left of the treated cells (red bar) and in a time-ascending order as indicated on top of the image in (A). Three hundred thirty two clones were up-regulated or down-regulated after exposure to 50 μ M doxazosin. B–F are zoomed images of clusters of genes whose expression was regulated by doxazosin. The gene tree shown at the left of the images corresponds to the degree of similarity (Pearson correlation) of the pattern of expression for genes across the experiments. B: Genes down-regulated by doxazosin; (C–F), genes up-regulated by doxazosin. The degree of color saturation corresponds to the ratio of gene expression shown at the bottom of the image. [Color figure can be viewed in the online issue, which is available at www.interscience.wiley.com.]

TABLE I. Genes With Significant Changes in Expression in Response to Doxazosin After 8 hr

Gene symbol	Fold change		Gene symbol	Fold change		Gene symbol	Fold change	
	Normal	BPH		Normal	BPH		Normal	BPH
Upregulated genes								
Cell proliferation/cell cycle/apoptosis								
TNFAIP3	11.23	8.77	INHBA*	3.55	3.41	FTH1	3.68	1.83
INSIG1	9.72	8.69	BCL2A1*	3.57	2.05	CKS2	3.17	2.48
GEM2*	8.60	4.53	IL11*	2.87	3.80	FOSL1*	1.97	2.94
IL6*	9.96	5.63	CED-6	3.52	1.95	RASD1*	1.41	3.77
FOS*	9.18	4.63	DDIT3*	3.82	2.58	MYC*	2.22	2.34
BIRC3*	6.28	3.43	CDK5R1	2.66	3.01	CXCL1*	2.90	1.29
IER3	6.89	3.72	CNK	3.10	3.04	TM4SF1	3.17	1.46
LIF*	4.17	4.68	FOSB*	2.60	2.76	PHLDA1	1.82	2.20
OLK38	5.43	5.33	NFKBIA*	1.32	2.17			
Immune/defense/stress response								
PTGS2	16.91	5.70	CXCL2*	7.31	2.31	TNFAIP6*	2.29	1.26
GEM2*	8.60	4.53	BCL2A1*	3.57	2.05	SGK	5.67	1.57
IL6*	9.25	5.58	CCL20*	3.67	1.50	FOSL1*	1.97	2.94
FOS*	9.18	4.63	DUSP10*	2.71	2.79	CXCL1*	2.90	1.29
HSPA6	2.31	1.62	DDIT3*	3.82	2.58	DNAJB1	1.15	2.14
CSF2*	2.45	3.64	CEBPB*	4.27	2.70			
Cell-cell signaling/signal transduction								
CXCL3	17.76	4.56	INHBA*	3.55	3.41	RASD1*	1.41	3.77
NR4A1	9.35	6.08	IL11*	2.87	3.80	CXCL1*	2.90	1.29
GEM2*	8.60	4.53	CCL20*	3.67	3.80	EDN3	2.60	1.39
IL6*	9.96	5.63	DUSP10*	2.71	2.79	GNA13	2.31	2.10
BIRC3*	6.28	3.43	RRAD	4.04	2.91	DPYSL3	1.47	2.64
CSF2*	2.45	3.64	BMP2	2.40	2.84	TTRAP	2.14	1.59
CXCL2*	7.31	2.31	SPRY2	1.78	3.99	TNFAIP6*	2.29	1.26
DUSP5	5.13	4.30	WISP3	3.59	2.56			
Transcriptional regulation								
FOS*	9.18	4.63	COPEB	2.94	4.35	MAFF	2.03	2.17
LIF*	4.17	4.68	MSC	2.80	4.35	MYC*	2.22	2.34
EGR1	4.15	5.55	DDIT3*	3.82	2.58	NR1D1	2.62	1.91
PLAB	6.99	2.09	CEBPB*	4.27	2.70	SNAI2	1.75	2.79
CRYPTIC	4.29	3.23	FOSB*	2.60	2.76	PMX1	2.69	1.80
ATF3	3.35	3.19	WTAP	4.00	2.20	FOSL1*	1.97	2.94
JUNB	4.09	3.91	JUN	2.73	4.23	JUND	2.90	2.48
Other biological processes								
HMOX1	23.46	7.51	LDLR	3.32	2.45	CLN8	1.99	2.86
GLS	7.92	3.59	DYRK3	2.89	2.91	SLC2A3	2.37	1.95
DCT	3.48	4.50	HRY	1.41	2.20	AKR1B10	2.31	1.97
SLC19A2	5.10	2.31	TERF2IP	2.67	3.65	PIM1	1.86	1.80
HMGCS1	4.61	4.38	BHLHB2	3.17	3.17	COL4A3BP	2.56	1.43
FBXO32	7.86	2.54	SLC16A6	2.05	2.59	AKR1C1	3.07	1.22
SCD	4.24	2.13	NPC1	3.02	1.86			
			SAT	2.51	2.36			
Downregulated genes								
CYP1B1	3.06	2.03	SFTPC	5.26	3.85	TXNIP	7.20	4.10

*Genes appear under more than one category.

TABLE II. Validation of Gene Expression Changes Using Real-Time RT-PCR

Sample gene	BPH1_8 hr		BPH2_8 hr		TZ1_8 hr		TZ2_8 hr	
	RT-PCR	Array	RT-PCR	Array	RT-PCR	Array	RT-PCR	Array
<i>EGR1</i> ↑	6.65 ± 1.36	8.63	3.40 ± 1.40	2.46	3.17 ± 1.18	5.82	2.24 ± 1.28	2.48
<i>TNFAIP3</i> ↑	21.60 ± 1.80	11.57 ± 2.67	8.19 ± 1.55	5.97 ± 0.77	11.06 ± 1.20	17.35 ± 2.63	3.82 ± 1.13	5.11 ± 0.39
<i>IL6</i> ↑	19.25 ± 1.86	4.93	11.06 ± 1.53	6.32	29.86 ± 1.18	13.64	13.00 ± 1.09	6.28
<i>HMOX1</i> ↑	2.24 ± 1.97	2.97	15.63 ± 1.70	12.04	17.96 ± 1.23	30.91	18.38 ± 1.15	16
<i>JUNB</i> ↑	5.92 ± 1.80	5.59 ± 0.42	1.07 ± 1.58	2.23 ± 0.29	3.32 ± 1.43	5.91 ± 0.42	2.89 ± 1.16	2.26 ± 0.07
<i>INSIG1</i> ↑	17.55 ± 1.82	8.88 ± 0.52	20.16 ± 1.58	8.52 ± 0.50	7.64 ± 1.29	9.48 ± 1.11	5.28 ± 1.39	9.96 ± 0.44
<i>GADD45B</i>	3.48 ± 1.81↑	3.22 ± 1.48↑	1.17 ± 1.57↓	1.17 ± 0.18↑	1.23 ± 1.23↓	1.11 ± 0.15↓	1.96 ± 1.23↓	1.56 ± 0.04↓
<i>TXNIP</i> ↓	3.25 ± 0.56	2.88 ± 0.10	3.82 ± 0.65	5.32 ± 0.05	12.70 ± 0.78	9.15 ± 0.04	9.62 ± 0.89	5.24 ± 0.01
<i>CYP11B1</i> ↓	1.87 ± 0.57	1.97 ± 0.467	1.74 ± 0.66	2.08 ± 0.54	4.39 ± 0.83	3.03 ± 0.24	3.73 ± 0.94	3.09 ± 0.18
<i>SFTPC</i> ↓	1.20 ± 0.49	2.91	3.65 ± 0.60	4.96	2.19 ± 0.79	7.01	6.65 ± 0.50	3.76

Bold entries indicate the only pair of data that showed expression changes in different directions in the RT-PCR vs. the microarray analyses.

TGF-β as a Molecular Target of Doxazosin

Since other investigators have suggested that apoptosis induced by doxazosin is mediated by the induction of TGF-β [3], we examined our data for evidence to support this theory. Although TGF-β sequences were present on the array, gene expression of TGF-β was not changed by treatment with doxazosin in either normal or BPH stromal cells. Therefore, at least at the RNA level, TGF-β did not appear to be a molecular target of doxazosin. We also searched our data for indirect evidence of activity of TGF-β in doxazosin-treated cells. In a separate project, we had previously treated the normal and BPH stromal cells used in this study (F-TZ-55 and F-BPH-32) with 1 ng/ml of TGF-β and identified the regulated genes by cDNA microarray analysis using similar methodologies to those used in the present study. We, therefore, compared the genes regulated by TGF-β in that analysis with those regulated by doxazosin in the current study. The genes regulated in common by TGF-β and doxazosin are shown in Figure 3. There were 22 genes regulated in common by the two factors, suggesting only a limited degree of overlap (for full list of genes, see web supplement (<http://www.stanford.edu/~hongjuan/Doxazosin/>)).

TGF-β Does Not Mediate Doxazosin-Induced Apoptosis in Prostatic Stromal Cells

The small number of genes regulated in common by TGF-β and doxazosin in normal and BPH stromal cells in our microarray analyses did not strongly support a role for TGF-β as a key mediator of apoptosis in response to doxazosin. To explore this further, we tested whether blocking TGF-β could block apoptosis in doxazosin-treated stromal cells by monitoring collapse of the mitochondrial membrane potential as an early event during apoptosis. At 24 hr, doxazosin caused a

72% decrease in membrane potential compared to diluent-treated control cells (Fig. 4). This decrease in membrane potential was not significantly changed by co-treatment with either pan-neutralizing antibody against TGF-β (10 µg/ml) or non-immune IgG (Fig. 4).

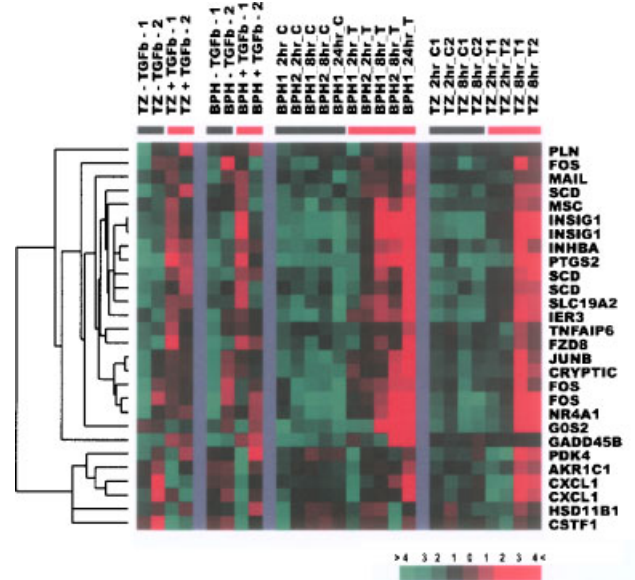


Fig. 3. TGF-β-responsive genes modulated by doxazosin. Doxazosin-regulated genes were compared with a set of TGF-β-responsive genes identified previously. The effect of doxazosin on expression of the genes in common is shown to the right organized in the same order as in Figure 1A. The effect of TGF-β is shown to the left with untreated cells (black bar) and treated cells (red bar) in duplicates for both BPH and normal stromal cells. The gene tree shown at the left of the images corresponds to the degree of similarity (Pearson correlation) of the pattern of expression for genes across the experiments. The degree of color saturation corresponds with the ratio of gene expression shown at the **bottom** of the image. [Color figure can be viewed in the online issue, which is available at www.interscience.wiley.com.]

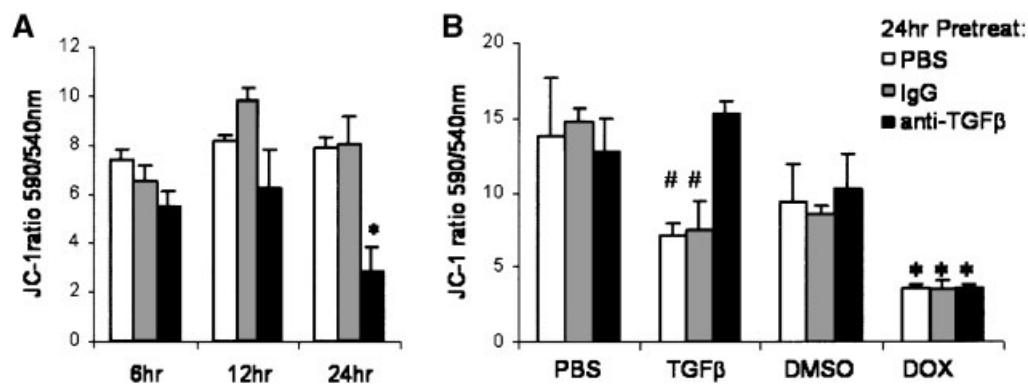


Fig. 4. Measurement of stromal cell mitochondrial membrane potential ($\Delta\Psi$) following doxazosin or TGF- β treatment. **A:** JC-1 fluorescence measurement of $\Delta\Psi$ after treatment with five (shaded bars) or 50 (solid bars) μM doxazosin compared to control (open bars). Error bars represent standard deviation of triplicate wells; *, $P < 0.05$. **B:** JC-1 fluorescence measurement of cells treated with doxazosin (50 μM) or its diluent DMSO (0.1%), or TGF β (10 ng/ml) or its diluent PBS, following a 24 hr pretreatment with PBS, IgG (10 $\mu\text{g}/\text{ml}$) or anti-TGF- β neutralizing antibody (10 $\mu\text{g}/\text{ml}$). Representative data from three separate experiments; error bars represent standard deviation of triplicate wells; ##, $P < 0.05$ TGF- β_1 versus PBS treatment; * $P < 0.05$ doxazosin versus DMSO treatment.

Addition of exogenous TGF- β itself induced apoptosis (decreased membrane potential by 45% compared to diluent-treated control cells), but only at the high concentration of 10 ng/ml (Fig. 4). Neutralizing antibody against TGF- β (10 $\mu\text{g}/\text{ml}$) blocked TGF- β -induced decrease in membrane potential, whereas 10 $\mu\text{g}/\text{ml}$ of non-immune IgG did not (Fig. 4). Altogether, these results do not support the concept that induction of TGF- β by doxazosin mediates doxazosin-induced apoptosis in prostatic stromal cells.

TNF- α Implicated as a Mediator of Doxazosin Activity

Many of the genes regulated by doxazosin in the normal and BPH stromal cells pointed to activation of a TNF- α signaling pathway. The gene most highly up-regulated by doxazosin in both types of cells was TNF- α -induced protein 3 (TNFAIP3), whose expression is known to be rapidly induced by TNF- α [11]. Other genes up-regulated by doxazosin—IL-6, EGR-1, and JunB—are also known targets of TNF- α [11]. However, TNF- α itself was not among the genes whose expression was altered by doxazosin treatment in our microarray analysis. To determine whether postranscriptional events might lead to elevated TNF- α protein but not RNA in response to doxazosin, we measured TNF- α protein secreted by cells using a sensitive ELISA method. Replicating the conditions used for the microarray analyses, cells were fed fresh medium two days prior to the addition of 50 μM doxazosin or diluent. Levels of TNF- α protein were measured in conditioned media taken 24 and 48 hr later. No measurable TNF- α was found in conditioned media from either treated or untreated cells, ruling out an increase in TNF- α protein in response to doxazosin.

Doxazosin Increased ROS in Prostatic Stromal Cells

Even though TNF- α itself was not identified as a molecular target of doxazosin, our microarray results nevertheless suggested the involvement of a TNF- α -related signaling pathway in doxazosin-induced apoptosis. Generation of ROS is commonly associated with such a signaling pathway, so we evaluated the ability of doxazosin to increase the level of ROS in prostatic stromal cells. Cellular H_2O_2 levels in doxazosin-treated relative to untreated cells increased significantly in a dose-dependent manner at 6 hr (Fig. 5). This result suggests that ROS may trigger the subsequent downstream genetic and biological events occurring in stromal cells in response to doxazosin, including the induction of a TNF- α -related signaling pathway.

DISCUSSION

We have systematically examined the doxazosin-induced gene expression changes in normal and BPH stromal cells using cDNA microarrays, and identified potential molecular targets of doxazosin in these two cell types. Hierarchical clustering analysis revealed striking gene expression variations in response to doxazosin in common between both normal and BPH stromal cells. One hundred fifteen genes identified by SAM analysis showed significant differential expression after doxazosin treatment. The known functions of 67 of these genes indicate that doxazosin may express its activities by modulating a variety of biological processes such as cell proliferation/apoptosis, immune defense, cell-cell signaling/signal transduction, and transcription activity. It is interesting to note that the majority of doxazosin-responsive genes were up-

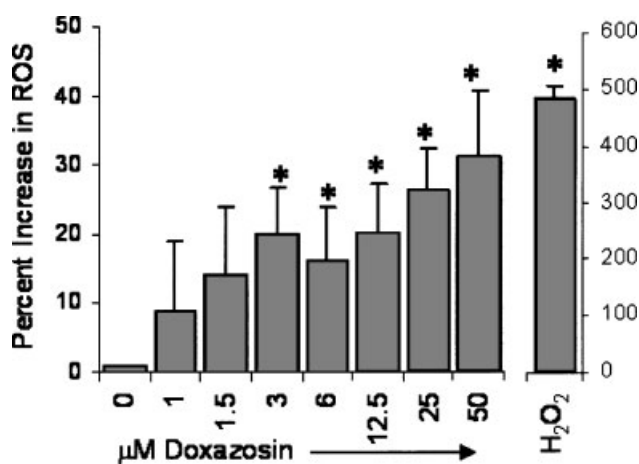


Fig. 5. CM-H₂DCFDA fluorescence determination of ROS levels in stromal cells after exposure to doxazosin for 6 hr. ROS after hydrogen peroxide (500 μM) is shown as a positive control. Data is shown as a percent increase in fluorescence compared to DMSO treatment. Representative data from two separate experiments; error bars represent standard deviation of triplicate wells; *, $P < 0.05$.

regulated and less than 5% were down-regulated. However, the functions of genes that showed decreased expression after treatment may point to biological mechanisms that underlie doxazosin activity in BPH as well as potential activity against prostate cancer. For example, one of the down-regulated genes, *CYP1B1*, encodes an enzyme that activates procarcinogens [12]. A number of cancer chemopreventive agents, including selenium and resveratrol, decrease *CYP1B1* gene expression (our unpublished data and [13]). Therefore, doxazosin, like these other agents, may protect against carcinogenicity induced by compounds that undergo *CYP1B1*-catalyzed bioactivation.

Doxazosin also decreased expression of TXNIP in prostatic stromal cells. TXNIP binds and inhibits thioredoxin, one of the primary components of the thiol-reducing systems that maintain a reduced intracellular state [14]. Since, we observed that doxazosin treatment quickly increased ROS, the decreased expression of TXNIP possibly represents a feedback mechanism to maintain cellular redox homeostasis.

We also identified genes that were differentially regulated by doxazosin in BPH versus normal stromal cells. This may reflect the different basal transcriptome between the two cell types upon which doxazosin action was superimposed. Our finding that hierarchical clustering of gene expression between normal and BPH cells completely separated the two types of cells supports previous reports, by us and others, of BPH-specific biological traits of cultured prostatic stromal cells [4]. Further investigation of these genetic differences may provide insight into the etiology of BPH and be relevant to the clinical activity of drugs such as doxazosin that are used to treat BPH.

Results from several previous studies implicated TGF- β as a mediator of doxazosin- or terazosin-induced apoptosis. In the mouse prostate reconstitution model, doxazosin increased apoptosis in conjunction with up-regulation of TGF- β_1 protein expression [15]. Immunohistochemical analyses of BPH tissues from men treated with finasteride and with or without terazosin revealed increased expression of TGF- β_1 in both the epithelium and stroma of terazosin-treated men [3]. In the aforementioned studies, it was not determined whether up-regulation of TGF- β_1 occurred at the transcriptional or posttranscriptional level. In examining our results, TGF- β was not among the genes regulated by doxazosin in our microarray analyses. The absence of TGF- β_1 in the list of genes up-regulated at the transcription level did not rule out the involvement of TGF- β_1 protein in doxazosin action. However, we did not find that neutralizing antibody against TGF- β blocked the apoptotic effects of doxazosin on these cells, showing that TGF- β protein did not mediate apoptosis. This result differs from that of Ilio et al., who concluded from a similar study that doxazosin-induced apoptosis in cultured prostatic stromal cells was mediated in part by autocrine production of TGF- β [16]. However, these investigators showed that neutralizing antibody against TGF- β caused only a modest decrease in doxazosin-induced apoptosis. Moreover, the level of TGF- β production by these cells in the presence of doxazosin was significantly less than that shown to be required to induce apoptosis in these cells. We conclude that TGF- β is not a key mediator of apoptosis in prostatic stromal cells in response to doxazosin.

While the mechanism by which doxazosin induces apoptosis is unknown, Benning et al. proposed that doxazosin and terazosin may cause severe perturbations in cellular attachment to extracellular matrix, resulting in anoikis [17]. While these investigators implicated activation of the TGF- β signaling pathway in this process, our results are not consistent with a role for TGF- β . Recently Keledjian and Kyprianou showed that treatment of the prostate cancer cell line, PC-3, with doxazosin for 24 hr decreased the ability of the cells to reattach after detachment from the substrate [18]. While this is interesting, it does not in fact demonstrate anoikis, which is apoptosis induced by loss of attachment to extracellular matrix. Levels of vascular endothelial growth factor (VEGF) RNA were also decreased by doxazosin treatment of PC-3 cells in this study, which we did not observe in the prostatic stromal cells. In fact, in a limited cDNA microarray analysis of doxazosin-treated PC-3 cells, with arrays consisting of only 23 genes [19], the genetic program initiated by doxazosin did not show substantial overlap with that found by us in prostatic stromal cells, suggesting cell type-specific activity of doxazosin.

While gene expression profiles induced by the identical stimulus may vary considerably among different types of cells, it is informative to compare the genes that were noted to differ between anchored and non-anchored (undergoing anoikis) mammary cancer cells (MCF-7) and genes regulated by doxazosin in prostatic stromal cells. In the experiments with MCF-7 cells, EGR1 was completely suppressed by anchorage, leading the investigators to speculate that EGR1 might induce TRAIL production in non-anchored cells [20]. EGR1 was among the genes up-regulated by doxazosin in our study (5.6-fold in BPH cells and 4.2-fold in normal cells), consistent with the possible induction of anoikis by doxazosin. Heme oxygenase (HMOX1) was also suppressed by anchorage of MCF-7 cells, and HMOX1 was induced by doxazosin in prostate cells (7.5-fold in BPH cells and 23.5-fold in BPH cells). Apoptosis in non-anchored MCF-7 cells was seemingly mediated by TRAIL, but we saw no induction of TRAIL by doxazosin in prostatic stromal cells.

Although the pattern of genes that we observed to be regulated by doxazosin in prostatic stromal cells implicated TNF- α in doxazosin-induced apoptosis, TNF- α itself was not among the genes whose expression was altered by doxazosin treatment in our microarray analysis. We also did not detect TNF- α protein in cell culture media during treatment with doxazosin, ruling out a postranslational mechanism of increased expression of TNF- α protein in response to doxazosin. Nonetheless, our results indicate a potential role of a TNF- α -like signaling pathway in doxazosin-induced apoptosis whose validity still requires further studies. In addition, we found that treatment of prostatic stromal cells with doxazosin quickly generated ROS in a dose-dependent manner. ROS may provide the initial stimulus triggering a TNF- α -related signaling pathway that leads to cell death, or may be the consequence of TNF- α -related signaling.

In summary, we have identified potential molecular targets of doxazosin in normal and BPH stromal cells on a genome-wide scale using cDNA microarrays. Our results do not support the involvement of TGF- β in doxazosin-induced apoptosis, but rather suggest a role for a TNF- α -related signaling pathway. Our data set will not only provide clues for future studies on the mechanism of doxazosin-induced apoptosis but may also lead to improved therapies for BPH based on mechanistic knowledge.

REFERENCES

- Oesterling JE. Benign prostatic hyperplasia: A review of its histogenesis and natural history. *Prostate Suppl* 1996;6:67-73.
- Kirby RS, Pool JL. Alpha adrenoceptor blockade in the treatment of benign prostatic hyperplasia: Past, present, and future. *Br J Urol* 1997;80:521-532.
- Kyprianou N. Doxazosin and terazosin suppress prostate growth by inducing apoptosis: Clinical significance. *J Urol* 2003;169:1520-1525.
- Peehl DM, Sellers RG. Cultured stromal cells: An in vitro model of prostatic mesenchymal biology. *Prostate* 2000;45:115-123.
- Zhao H, Whitfield ML, Xu T, Botstein D, Brooks JD. Diverse effects of methylseleninic acid on the transcriptional program of human prostate cancer cells. *Mol Biol Cell* 2004;15:506-519.
- Sherlock G, Hernandez-Boussard T, Kasarskis A, Binkley G, Matese JC, Dwight SS, Kaloper M, Weng S, Jin H, Ball CA, Eisen MB, Spellman PT, Brown PO, Botstein D, Cherry JM. The Stanford Microarray Database. *Nucleic Acids Res* 2001;29:152-155.
- Eisen MB, Spellman PT, Brown PO, Botstein D. Cluster analysis and display of genome-wide expression patterns. *Proc Natl Acad Sci USA* 1998;95:14863-14868.
- Tusher VG, Tibshirani R, Chu G. Significance analysis of microarrays applied to the ionizing radiation response. *Proc Natl Acad Sci USA* 2001;98:5116-5121.
- Weitsman GE, Ravid A, Liberman UA, Koren R. Vitamin D enhances caspase-dependent and -independent TNF α -induced breast cancer cell death: The role of reactive oxygen species and mitochondria. *Int J Cancer* 2003;106:178-186.
- Whitfield ML, Sherlock G, Saldanha AJ, Murray JJ, Ball CA, Alexander KE, Matese JC, Perou CM, Hurt MM, Brown PO, Botstein D. Identification of genes periodically expressed in the human cell cycle and their expression in tumors. *Mol Biol Cell* 2002;13:1977-2000.
- Zhou A, Scoggin S, Gaynor RB, Williams NS. Identification of NF-kappa B-regulated genes induced by TNF α utilizing expression profiling and RNA interference. *Oncogene* 2003;22:2054-2064.
- McFadyen MC, Rooney PH, Melvin WT, Murray GI. Quantitative analysis of the Ah receptor/cytochrome P450 CYP1B1/CYP1A1 signalling pathway. *Biochem Pharmacol* 2003;65:1663-1674.
- Surh YJ, Hurh YJ, Kang JY, Lee E, Kong G, Lee SJ. Resveratrol, an antioxidant present in red wine, induces apoptosis in human promyelocytic leukemia (HL-60) cells. *Cancer Lett* 1999;140:1-10.
- Nordberg J, Arner ES. Reactive oxygen species, antioxidants, and the mammalian thioredoxin system. *Free Radic Biol Med* 2001;31:1287-1312.
- Yang G, Timme TL, Park SH, Wu X, Wyllie MG, Thompson TC. Transforming growth factor beta 1 transduced mouse prostate reconstitutions: II. Induction of apoptosis by doxazosin. *Prostate* 1997;33:157-163.
- Ilio KY, Park II, Pins MR, Kozlowski JM, Lee C. Apoptotic activity of doxazosin on prostate stroma in vitro is mediated through an autocrine expression of TGF-beta1. *Prostate* 2001;48:131-135.
- Benning CM, Kyprianou N. Quinazoline-derived alpha1-adrenoceptor antagonists induce prostate cancer cell apoptosis via an alpha1-adrenoceptor-independent action. *Cancer Res* 2002;62:597-602.
- Keledjian K, Kyprianou N. Anoikis induction by quinazoline based alpha 1-adrenoceptor antagonists in prostate cancer cells: Antagonistic effect of bcl-2. *J Urol* 2003;169:1150-1156.
- Partin JV, Anglin IE, Kyprianou N. Quinazoline-based alpha 1-adrenoceptor antagonists induce prostate cancer cell apoptosis via TGF-beta signalling and I kappa B alpha induction. *Br J Cancer* 2003;88:1615-1621.
- Goldberg GS, Jin Z, Ichikawa H, Naito A, Ohki M, El-Deiry WS, Tsuda H. Global effects of anchorage on gene expression during mammary carcinoma cell growth reveal role of tumor necrosis factor-related apoptosis-inducing ligand in anoikis. *Cancer Res* 2001;61:1334-1337.

Genome-Wide Characterization of Gene Expression Variations and DNA Copy Number Changes in Prostate Cancer Cell Lines

Hongjuan Zhao,¹ Young Kim,² Pei Wang,³ Jacques Lapointe,¹ Rob Tibshirani,^{3,4} Jonathan R. Pollack,² and James D. Brooks^{1*}

¹Department of Urology, Stanford University School of Medicine, Stanford, California

²Department of Pathology, Stanford University School of Medicine, Stanford, California

³Department of Statistics, Stanford, California

⁴Department of Health Research and Policy, Stanford University School of Medicine, Stanford, California

BACKGROUND. The aim of this study was to characterize gene expression and DNA copy number profiles in androgen sensitive (AS) and androgen insensitive (AI) prostate cancer cell lines on a genome-wide scale.

METHODS. Gene expression profiles and DNA copy number changes were examined using DNA microarrays in eight commonly used prostate cancer cell lines. Chromosomal regions with DNA copy number changes were identified using cluster along chromosome (CLAC).

RESULTS. There were discrete differences in gene expression patterns between AS and AI cells that were not limited to androgen-responsive genes. AI cells displayed more DNA copy number changes, especially amplifications, than AS cells. The gene expression profiles of cell lines showed limited similarities to prostate tumors harvested at surgery.

CONCLUSIONS. AS and AI cell lines are different in their transcriptional programs and degree of DNA copy number alterations. This dataset provides a context for the use of prostate cancer cell lines as models for clinical cancers. *Prostate* 63: 187–197, 2005. © 2004 Wiley-Liss, Inc.

KEY WORDS: androgen; microarray; aCGH; tumor subtypes; metastasis; prostate cancer cell lines

INTRODUCTION

The high incidence of prostate cancer, the most common cancer in American men, demands the development of novel therapeutic strategies which will be achieved through a better understanding of the molecular events underlying the initiation and progression of prostate cancer [1,2]. Prostate cancer-derived cell lines have been used as important model systems to study the molecular mechanisms of prostate cancer for several decades, yielding a large amount of valuable information on tumorigenesis and progression, and serving as models for the development of new treatment strategies [3]. Prostate cancer cell lines are classified as either androgen sensitive (AS), which express the androgen receptor (AR) and androgen-responsive genes such as *PSA*, and androgen insensitive (AI), which lack AR and do not respond to

androgen stimulation. In general, AS prostate cancer cells have a lower malignant potential than AI cells [4,5].

Despite the wide usage of these cell lines in prostate cancer research, a global genotypic and phenotypic characterization of these cell lines is currently lacking. More importantly, how well these cell lines model primary or metastatic tumors, as reflected in their

Grant sponsor: NIH; Grant number: U01CA85129.

*Correspondence to: James D. Brooks, Department of Urology, Stanford Medical Center, 300 Pasteur Drive, Grant Building S287, Stanford, CA 94305. E-mail: jdbrooks@stanford.edu

Received 17 May 2004; Accepted 22 June 2004

DOI 10.1002/pros.20158

Published online 14 October 2004 in Wiley InterScience (www.interscience.wiley.com).

global transcriptional programs, is unknown and could help in assessing the validity of experiments that use these cell lines. Here, we characterize the gene expression and DNA copy number profiles of five AS (LNCaP, LAPC-4, MDA PCa 2a, MDA PCa 2b, and 22Rv1) and three AI (PC-3, PPC-1, and DU 145) prostate cell lines using DNA microarrays. Comparison of these profiles reveals consistent differences between AS and AI cell lines, while comparison of the cell line transcript profiles to those from clinical samples allows assessment of the fidelity of the prostate cancer cell lines to the disease in vivo.

MATERIALS AND METHODS

Cell Culture

LNCaP and 22Rv1 were obtained from the American Type Culture Collection (ATCC, Manassas, VA) and grown in RPMI 1640 with 2 mM L-glutamine, supplemented with 10% fetal bovine serum (FBS), 100 U/ml penicillin/100 µg/ml streptomycin (Invitrogen™, Carlsbad, CA). PC-3 and PPC-1 were a gift from William G. Nelson (Johns Hopkins University, Baltimore, MD) and grown in the same medium. LAPC-4 was a gift from Robert E. Reiter (University of California at Los Angeles, Los Angeles, CA) and cultured in Iscove's media with 10% FBS and 100 U/ml penicillin/100 µg/ml streptomycin. MDA PCa 2a and MDA PCa 2b were kindly provided by Nora Navonne (M.D. Anderson Cancer Center, Houston, TX) and cultured in BRFF-HPC1 media (AthenaES™, Baltimore, MD) with 10% FBS and 100 U/ml penicillin/100 µg/ml streptomycin. DU 145 was obtained from ATCC and grown in F15K minimum essential medium with 10% FBS and 100 U/ml penicillin/100 µg/ml streptomycin. Cells were routinely fed with fresh media and incubated in a 37°C incubator at 5% CO₂.

Genomic DNA and Total RNA Isolation

Cells were collected from 150 mm cell culture plate by trypsinization and washed with 1× PBS. Genomic DNA was isolated from cultured tumor cells and the white blood cells of a healthy male using a QIAamp Blood DNA Maxi kit (Qiagen, Valencia, CA) according to manufacturer's instructions. The concentration of genomic DNA was determined using an MBA 2000 spectrometer (Perkin Elmer, Boston, MA), and the quality of genomic DNA was assessed by electrophoresis.

Total RNA was isolated using TRIzol solution (Invitrogen™). Medium was aspirated from each 150 mm cell culture plate and 5 ml TRIzol solution was added. After 5 min of gentle agitation, lysates were extracted with chloroform, and the organic and aqueous layers were separated using Phase Lock Gel (Eppendorf®,

Westbury, NY). Total RNA was precipitated with isopropanol and further purified with an RNeasy mini kit (Qiagen). The concentration of total RNA was determined using an MBA 2000 spectrometer (Perkin Elmer), and the integrity of total RNA was assessed using a 2100 Bioanalyzer (Agilent Technologies, Palo Alto, CA).

Microarray Hybridization

Transcript profiling. Cy5 labeled cDNA was prepared from total RNA isolated from tumor cells and Cy3 labeled cDNA from total RNA of custom-made reference RNA pooled from 11 established human cell lines [6] by reverse transcription. Seventy micrograms of total RNA was mixed with 5 µg of oligo dT primer (Qiagen) in 16 µl of RNase-free water, incubated at 70°C for 10 min, and cooled on ice for 2 min. The remaining probe labeling, hybridization, and array washing were carried out as previously described [7]. The combined Cy5 and Cy3 labeled probes were hybridized to cDNA microarrays containing 41,805 elements representing 27,365 genes (Stanford Functional Genomics Facility). The raw data are available at http://www.stanford.edu/~hongjuan/prostate_cell_line.

Array-based comparative genomic hybridization (aCGH). Digestion, labeling, and microarray hybridization of genomic DNA from tumor cells and normal male blood cells were essentially performed as previously described with slight modification [8]. Four micrograms of genomic DNA was digested with *DpnII* and purified using Qiaquick PCR purification kit (Qiagen). Digested DNA from tumor cells was labeled by Cy5, and that from normal blood cells by Cy3 using a RadPrime DNA Labeling System (Invitrogen™) in a 50 µl reaction volume. The combined Cy5 and Cy3 labeled probes were hybridized to the same cDNA microarrays as used for transcript profiling described above. The raw data are available at http://www.stanford.edu/~hongjuan/prostate_cell_line.

Data Analysis

Arrays were scanned using an Axon scanner 4000B, and analyzed with GenePix Pro 3.0 software (Axon Instruments, Union City, CA). Spots of poor quality were removed from further analysis by visual inspection. The resulting data from each array was submitted to the Stanford Microarray Database (SMD <http://genome-www5.stanford.edu/microarray/SMD>) [9].

Identification of chromosomal regions with DNA copy number changes. Cluster along chromosomes (CLAC) was used to identify regions with statistically significant DNA copy number changes from the aCGH

data (<http://www-stat.stanford.edu/~wp57/CGH-Miner>) [10]. A tree is built using a hierarchical clustering algorithm along each chromosome arm where regions with DNA copy number gain or loss are separated into different branches. Whether a node (a point where two or more lines meet in a tree) is associated with DNA copy number change is determined based on the joint distribution of three statistics: the mean value of the leaves (the elements at the very bottom of a tree) of the sub-tree, the size of the sub-tree, and the height of this node in the tree. A false discovery rate (FDR) is defined for each cell line based on data from normal cells using an empirical Bayes approach. The selected regions with gain or loss and log₂ based ratios of DNA copy number in cell line versus normal blood cells for each gene are available at <http://www.stanford.edu/~hongjuan/prostate> cell line.

Analysis of transcript profiles. A hierarchical clustering algorithm was applied to group genes and samples on the basis of their similarities in expression, and the results were visualized using TreeView software (<http://rana.lbl.gov/EisenSoftware.htm>) [11]. Only spots with a signal intensity >50% above background in the Cy5 and Cy3 channels were retrieved. For the cell lines, data was included in the analysis if it was available in at least 70% of the samples. For combined analysis of the cell lines and tumor samples, only spots with a regression correlation (of intensity among all pixels within a spot) greater than 0.5 and measurable in at least 75% of the samples were included in the analysis. Fluorescence ratios were mean-centered for each gene across all samples included in each analysis.

Significance analysis for microarrays (SAM). Genes with potentially significant variations in expression between AS and AI cells were identified using the

SAM procedure [12], which computes a two-sample T-statistic (e.g., for AS vs. AI cells) for the normalized log ratios of gene expression levels for each gene. The procedure thresholds the T-statistics to provide a “significant” gene list and provides an estimate of the false-discovery rate (the percentage of genes identified by chance alone) from randomly permuted data. Clones (18,507) whose expression was available in at least 80% of the samples were included in the analysis. We used a selection threshold that gives the lowest FDR and identifies the highest number of significant genes.

RESULTS

Gene Expression Patterns of AS and AI Prostate Cancer Cells

To obtain a representative view of the gene expression profiles of prostate cancer cells, we measured transcript levels of 27,365 genes in five AS and three AI cell lines (Table I) using cDNA microarrays. Unsupervised hierarchical clustering analysis was used to group the eight cell lines based on the similarities in their expression patterns over 1,703 selected clones representing 1,261 unique genes that varied by at least 3-fold from the mean abundance in at least two cell lines (Fig. 1, for full list of clones, see web supplement at <http://www.stanford.edu/~hongjuan/prostate> cell line). All AS cell lines clustered separately from the AI cell lines (Fig. 1A), suggesting that AS cells share similar transcriptional programs that are different from AI cells. Out of the 1,261 genes, 420 showed differential expression between all AS and AI cells (e.g., Fig. 1B,C). The remaining 841 genes showed varied expression across the cell lines in ways not predicted by their AR status (Fig. 1A and supplemental website).

Expression of AR and its downstream targets accounted for some, but not all, of the differences in gene

TABLE I. Characteristics of Prostate Cancer Cell Lines Studied (Russell and Kingsley, 2003 [3])

Cell line	Source	Androgen sensitivity	Androgen receptor (AR)	PSA
LNCaP	Lymph node metastasis	Androgen sensitive (AS)	+	+
MDA 2a	Bone metastasis	AS	+	+
MDA 2b	Bone metastasis	AS	+	+
LAPC4	Lymph node metastasis	AS	+	+
22Rv1	Xenograft	AS	NR	+
PC-3	Lumbar metastasis	Androgen insensitive (AI)	–	–
PPC-1	Poorly differentiated adenocarcinoma	AI	–	–
DU 145	Central nervous system metastasis	AI	–	–

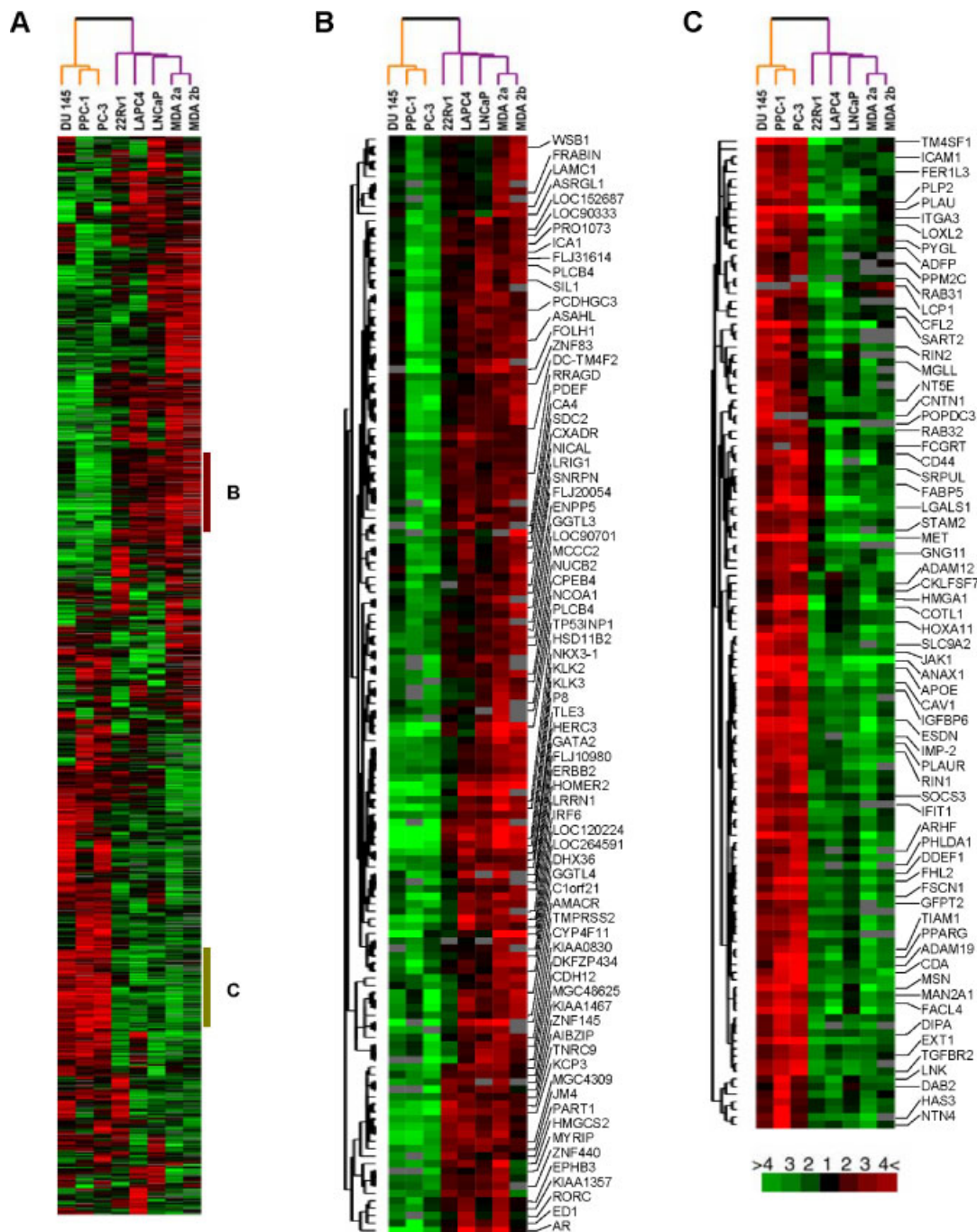


Fig. 1. Gene expression patterns between androgen sensitive (AS) and androgen insensitive (AI) cells shown by hierarchical clustering analysis. Both genes (represented by rows) and samples (represented by columns) were clustered according to their similarities in expression patterns. The degree of color saturation corresponds to the ratio of gene expression shown at the bottom of the image. In the dendrogram shown on **top** of the overview image (**A**), AS cells were colored purple and AI cells orange. The gene tree shown at the **left** of the images corresponds to the degree of similarity (Pearson correlation) of the pattern of expression for genes across the experiments. **B**: Genes down-regulated across AI cells but up-regulated across AS cells; **C**: genes up-regulated across AI cells but down-regulated across AS cells. [Color figure can be viewed in the online issue, which is available at www.interscience.wiley.com.]

expression between the AS and AI cell lines. AS cell lines expressed known androgen regulated genes [13–16], such as *NKX3-1*, *KLK2*, *KLK3*, *TMPRSS2*, and *AIBZIP* while AI cell lines expressed negligible levels of

these transcripts (Fig. 1B). We compared the cell line gene expression dataset to 385 named unique genes found to be responsive to androgen in LNCaP cells [17]. Out of the 420 genes that differentially expressed

between all AS and AI cells, only 22 were found in the androgen-responsive gene list, and out of the 1,261 genes that varied across all cell lines, 58 were found in this list (Fig. 2). The slight enrichment of androgen-responsive genes in these 420 and 1,261 genes (1.35- and 1.18-fold, respectively) was not statistically significant. To further assess the contribution of androgen signaling pathways to the differences in gene expression between AS and AI cells, we used SAM procedure to identify 1,248 transcripts representing 734 named unique genes whose expression level differed significantly between AS and AI cells with a FDR 0.5%. Thirty

nine out of these 734 genes were found in the androgen-responsive gene list, representing a 1.4-fold enrichment that is small but statistically significant ($P = 0.03$). The top 79 genes were listed according to their functions annotated in GO (Table II) [18]. Taken together, these results suggest that differential expression of androgen-responsive genes contribute to differences in expression profiles between AS and AI cells but to a limited degree.

Other than the androgen signaling pathway, genes differentially expressed between AS and AI cell lines are involved in diverse cellular processes based on their GO annotations [18]. For instance, AS cells showed relatively high levels of expression of genes involved in cell proliferation/apoptosis (*DAPK1*, *CCNG2*, *RRAGD*, *ERBB2*, *DHX36*, *AMACR*), cellular metabolism (*ASRGL1*, *PLCB4*, *CA4*, *ENPP5*, *GGTL3*, *MCCC2*, *HSD11B2*), and transcriptional regulation (*PDEF*, *NCOA1*, *TLE3*, *IRF6*, *GGTL4*, *MGC48625*, *TNRC3*, *ZNF440*, *RORC*). On the other hand, in AI cells higher levels of expression were noted in a set of genes implicated in the regulation of cell adhesion (*ICAM1*, *PLAU*, *ITGA3*, *LOXL2*, *LCP1*, *CFL2*, *CNTN1*, *LGALS1*, *ADAM12*, *COTL1*, *CAV1*, *PLAUR*, *FSCN1*, *ADAM13*, *MSN*), cell growth/maintenance (*TM4SF1*, *PLAU*, *MET*, *IGFBP6*, *PLAUR*, *SOCS3*, *EXT1*, *DAB2*), and immune response (*SART2*, *MGLL*, *FCGRT*, *APOE*, *IFIT1*).

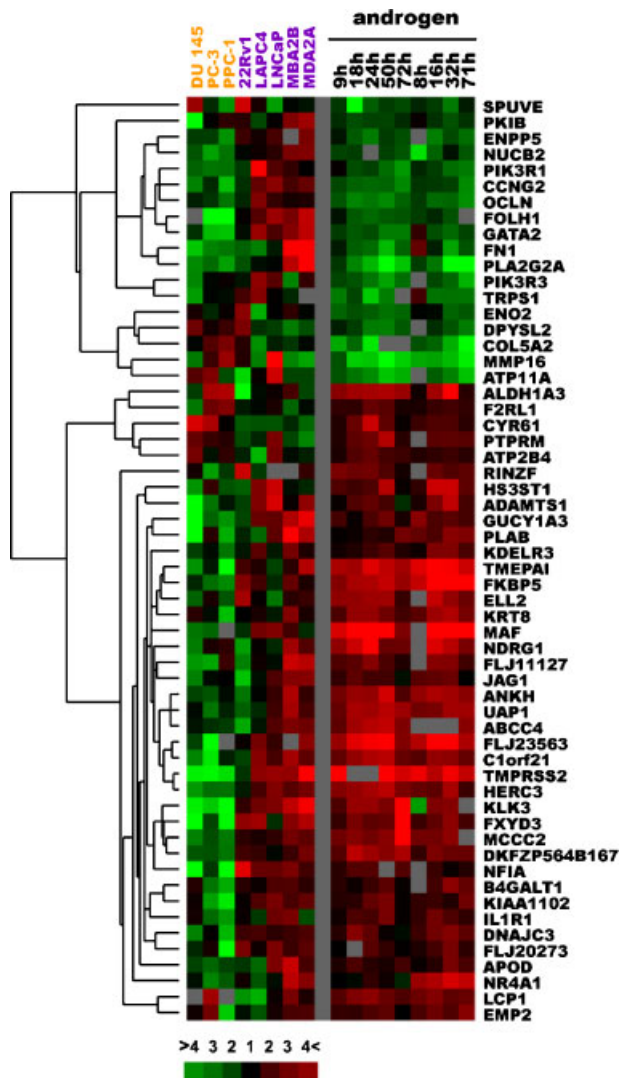


Fig. 2. Androgen-responsive genes differentially expressed in AS and AI cells. On the **left** are expression patterns of 58 androgen-responsive genes in the 8 cell lines. On the **right** are gene expression patterns of the same set of genes from two separate time courses induced by treatment of LNCaP cells with the synthetic androgen R1881. The red dots indicate well-characterized androgen-regulated genes. [Color figure can be viewed in the online issue, which is available at www.interscience.wiley.com.]

DNA Copy Number Changes in Prostate Cancer Cells and Their Contribution to RNA Expression Variation

To further explore the global genomic differences in prostate cancer cell lines, we characterized DNA copy number variations by aCGH using the same cDNA microarray platform utilized for expression profiling. A ratio of DNA copy number in the cell lines compared to normal, diploid karyotype cells was calculated for each gene, and multiple chromosome regions with significant changes in DNA copy number were identified using CLAC (Fig. 3) [10]. In general, AI cells, particularly PC-3 and PPC-1, harbored more DNA copy number changes than AS cells. The total number of genes showing significant copy number variations in AI cells ranged from 7,005 to 9,900, while in AS cells the number ranged from 1,502 to 6,306, and the difference was statistically significant ($P = 0.01$). Gains exceeded losses in all of the cell lines (Table III). MDA PCa 2a and MDA PCa 2b showed the fewest changes and shared very similar profiles (gain/loss, distribution, and magnitude) (Fig. 3). PC-3 and PPC-1 also showed similar changes across all chromosomes (Fig. 3). The selected regions as well as the complete dataset are available at <http://www.stanford.edu/~hongjuan/prostate> cell line.

TABLE II. Top 79 Genes Significantly Differentially Expressed Between AS and AI Cells Identified by Significance Analysis for Microarrays (SAM) Analysis

	Up-regulated in AI cells
Regulation of transcription	BAPX1, ETS1, ^a HOXA11, MCM3, ^a NMI, ^a TAZ, UHRF1
Cell adhesion/extracellular matrix/cytoskeleton	CD58, ^a COL4A2, CORO1C, ^a COTL1, CYR61, ^{a,b} ESDN, ^a ICAMI, ITGB1, ^a LOXL2, MSN, PTPN12, RINI ^a
Immune response	CD58, ^a ETS1, ^a IFIT5, IL6, ^a NMI ^a
Cell cycle/apoptosis	CAV1, ^a CAV2, ^a CORO1C, ^a CYR61, ^a DTR, ^a ESDN, ^a ETS1, ^a EXT1, ^a IGFBP6, ^a IL18, ^a IL6, ^a MCM3, ^a PLAUA, ^a PLAU, ^a TGFBR2, TNFRSF1B
Signal transduction	CAV1, ^a CAV2, ^a CORO1C, ^a DTR, ^a EXT1, ^a GNG11, IGFBP6, ^a IL18, ^a IL6, ^a ITGB1, ^a JAK1, MET, NMI, ^a PLAUA, ^a PLAU, ^a RIN1, ^a TIAM1
Other functions	ADFP, ANXA1, APOE, CDA, DDEF1, DPP9, FACLA, FER1L3, HPCA, SES1, LOC254531, MAN2A1, NT5E, PDXK, TXNDC
Unknown functions	DIPA, FSCN1, GK003, KIAA1949, LOC285533, PALM2, PHLDA1, PYGL
	Down-regulated in AI cells
Regulation of transcription	UHRF1, CREB3L4, IRX3, ZNF440
Other functions	ERBB3, FLJ14681, ^b FOLH1, ^b KLK3, ^b MCCC2, ^b MYO6, P8, POLI, RoXaN, SELENBP1
Unknown function	AZGP1, C14orf45, MGC22960, FLJ33977, KIAA0346, KIAA0977, MGC4309, TLE3 ^b

^aGenes appear in more than one category.

^bGenes in common with androgen responsive genes identified using SAM by DePrimo et al. [1].

High-level copy number changes (>3-fold), particularly gains, comprised only a small portion of the variations among the prostate cell lines (Table III). PC-3 and PPC-1 accounted for the majority of the total high-level gains (97%), as well as 58% of the total high-level loss (>3-fold). DNA copy number changes correlated with expression variations greater than 3-fold in 11% of the genes in all of the cell lines. In general, this correlation was lowest in the AS cell lines and greatest in the PC-3 and PPC-1 cell lines, suggesting that DNA

copy number changes might contribute to expression variations of these cells to a greater extent than the other prostate cancer cell lines.

Gene Expression Patterns of Prostate Cancer Cell Lines and Tumors

We have recently employed the same DNA microarray platform used in this study to define three molecular subtypes of prostate cancer associated with

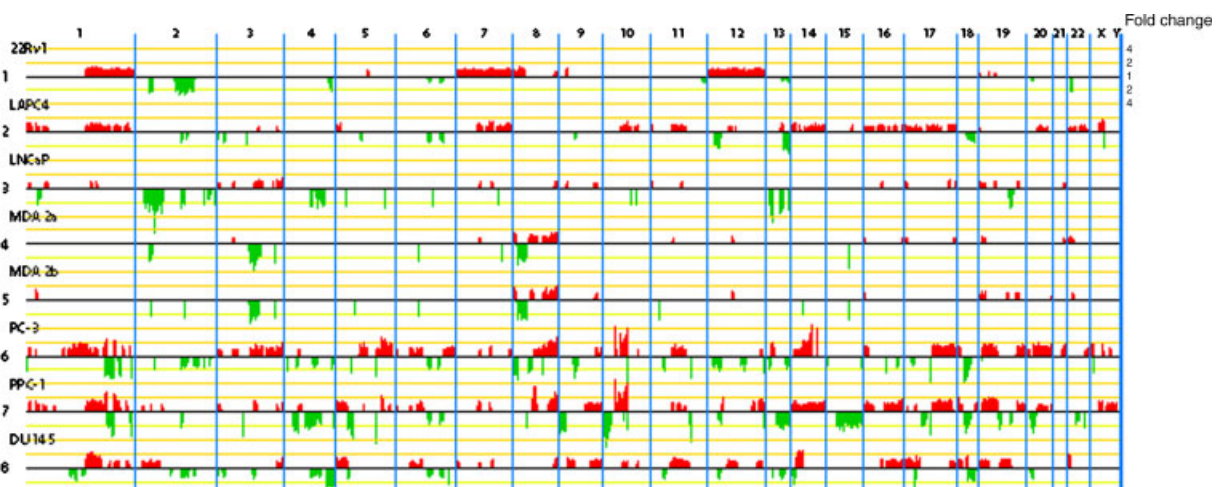


Fig. 3. DNA copy number changes in AS and AI prostate cancer cell lines. The chromosomal regions were separated by blue vertical lines and the chromosomal number was placed on top of the graph. Genes with DNA copy number gain were colored red and with loss green. The height of the bars represents the log₂ based ratio of DNA copy number changes. [Color figure can be viewed in the online issue, which is available at www.interscience.wiley.com.]

TABLE III. Comparison of DNA Copy Number Changes and RNA Expression Variations in Eight Cell Lines*

	22Rv1	LAPC4	LNCaP	MDA 2a	MDA 2b	Average	PC-3	PPC-1	DU 145	Average
Genes with DNA copy number changes										
↑	4,369	5,272	1,610	1,246	1,025	2,704 ^a	6,739	6,837	4,882	6,153 ^a
↓	1,094	1,034	984	596	477	837 ^b	2,372	3,063	2,123	1,500 ^b
High level DNA copy number changes (>3-fold)										
↑	0	2	0	0	1	<1 ^c	58	82	2	47 ^c
↓	13	13	88	43	31	38	117	180	25	107
High level RNA expression changes (>3-fold)										
↑	327	294	183	298	332	287	322	302	342	322
↓	233	241	187	268	214	229 ^d	259	375	299	311 ^d
RNA expression variation >3-fold associated with DNA copy number change										
↑	36 (11%)	47 (16%)	5 (3%)	7 (2%)	16 (5%)	22 (7% ^e)	88 (27%)	50 (17%)	46 (13%)	61 (19% ^e)
↓	5 (2%)	12 (5%)	8 (9%)	6 (2%)	9 (4%)	8 (4% ^f)	43 (17%)	39 (10%)	26 (9%)	36 (12% ^f)

*False discovery rate (FDR) <0.05 was chosen for all cell lines.

^{a-f}Differences observed in AS versus AI cells are statistically significant ($P < 0.05$).

distinct clinicopathological features [19]. To assess the similarities and differences between expression profiles of cell lines and the newly identified molecular subtypes of tumors, hierarchical cluster analysis was used to compare gene expression patterns of the 8 prostate cancer cell lines to 62 primary tumors and 9 pelvic lymph node metastases across 3,356 unique genes represented by 4,924 clones whose expression varied more than 3-fold in at least three samples (for full list of clones, see web supplement at [http://www.stanford.edu/~hongjuan/prostate cell line](http://www.stanford.edu/~hongjuan/prostate%20cell%20line)). In the dendrogram, tumors segregated into three distinct groups highly similar to that observed previously (types I, II, and III) (Fig. 4 and Lapointe et al. [19]). In addition, types I and II tumors were grouped on one main branch, while type III and cell lines on the other main branch, suggesting that cell lines may share more similarities with type III tumors than with types I and II tumors. Moreover, the AS and AI cell lines most closely resembled each other in their gene expression profiles, evidenced by the short branch length of the cluster dendrogram.

Hierarchical cluster analysis demonstrated that gene expression patterns of prostate cancer cell lines shared limited similarities to each of the three molecular tumor subtypes. For instance, genes such as *FGFR3*, *CLDN4*, and *TLE3* showed similar expression patterns in cell lines and type I tumors, a class comprised mainly of relatively low-grade, organ-confined tumors (Fig. 4B). In addition, genes such as *GTF2A1*, *PAI-RBP1*, *TFDP1*, *ILF2* that are involved in transcriptional regulation were expressed at high levels in cell lines and intermediate levels in most of type II tumors, but showed little expression in type III tumors (Fig. 4C). Both the cell lines and the type III tumors, comprised mainly

of lymph node metastases and a few high-grade primary tumors, showed high level expression of genes involved in protein synthesis (*RPL13*, *RPS9*, *RPL15*) and transcriptional regulation (*DRAP1*, *TRIM28*, *SELH*, *MA2*, *COBRA1*, *POLR2E*) (Fig. 4D), although the amplitude of the expression level of these genes in cell lines was relatively higher and more uniform than in lymph node metastases. Moreover, the AS cell lines expressed some genes (e.g., *STAT3*, *ITGAV*, *SNAP23*, *CD164*) at levels similar to those seen in type I and type II tumors, while these genes were not expressed in the type III tumors or in AI cell lines (Fig. 4F).

Cell lines did, however, show considerable differences in gene expression from each of the three molecular subtypes of tumors in hierarchical cluster analysis. For instance, all cell lines showed significantly higher expression levels of the proliferation genes (e.g., *CENPF*, *MCM4*, *CHEK1*, *MCM6*, *MCM3*, *CKS2*, *CDC6*, *CDC2*) compared to that observed in solid tumors (Fig. 4E). Removal of approximately 400 cell cycle regulated clones identified using results from previous study by Whitfield et al. [20] from the analysis did not alter significantly the overall cluster dendrogram (see web supplements). In addition, a host of extracellular matrix structural constituents, including different types of collagens (*COL18A1*, *COL4A2*, *COL1A1*, *COL5A1*, *COL16A1*, *COL6A3*, *COL1A*, *COL3A1*), showed high expression levels in lymph node metastases, lower expression in the primary tumors, and virtually absent expression in cell lines (see web supplement).

To further examine the relationships of cell lines and molecular subtypes of tumors in gene expression, we applied principle component analysis to the dataset. The projections of the 79 samples into the first three

principal components (pc1, pc2, and pc3), which capture 32.6, 43.2, and 49.6% of the variances in the dataset respectively, were plotted (Fig. 4G). Solid tumors most closely resemble each other in gene expression for pc1 and pc3, but not pc2. Cell lines are slightly closer to type III tumors in gene expression than to type I/II tumors for pc1. However, they closely resemble type I/II but not type III tumors for pc2. These results suggest that different subtypes of tumors shared similar gene expression with each other to a greater extent than with cell lines, although the cell lines do share some gene expression features with the solid tumors.

DISCUSSION

AS and AI prostate cancer cell lines have been discriminated from each other principally by their response to androgen stimulation, their expression of AR, and several androgen responsive genes such as *PSA*, and their growth kinetics. Global characterization of gene expression patterns and DNA copy number variations revealed two additional striking differences between AS and AI prostate cancer cell lines. First, there are intrinsic and reproducible differences in gene expression between AS and AI cell lines that involve genes from many functional classes beyond AR signaling pathways. Second, the AI cell lines show greater genome wide DNA copy number imbalances than the AS cell lines.

AR-signaling pathways are essential to prostate development, prostate carcinogenesis and progression [21]. With progression to androgen resistance, AR signaling remains intact, and virtually all tumors continue to express AR and *PSA*, despite absent ligand, possibly due to increased sensitivity to androgen or activation of signaling pathways downstream of AR [22–25]. In vitro, AS cell lines show expression of many androgen regulated genes, as well as many other genes not affected by androgen that are distinct from AI cell lines. Although AI cell lines do not express AR and *PSA*, they do, however, retain expression of a small set of genes identified as androgen responsive. It is possible that these remnants of the AR signaling pathway are necessary to allow AI cells to survive and proliferate. Furthermore, AI cells may require activation of other pathways outside of the androgen signaling pathway and this may account for the large differences in gene expression between AI and AS cells. Whether these changes are necessary for AI cell lines to survive without the androgen-signaling pathway intact is unclear, but could be a fruitful area of investigation.

A number of allelic imbalance events have been reported in primary human prostate cancers including

loss of chromosome material from 8p, 10q, 16q, 17p, and gain of chromosome 8q. While examples of each of these changes can be found in the cell lines, none of the cell lines shows all of these changes, and few have more than two of these changes. DNA copy number changes correlated with gene expression changes greater than 3-fold in only 11% of genes in the cell lines, suggesting that most alterations in transcript levels are not directly secondary to changes in DNA levels. Our findings are consistent with our prior observations of the effect of copy number changes on gene expression in breast cancers [26]. The AI cell lines had consistently more DNA copy number changes than the AS cell lines, and appear to have far more alterations, particularly gains, than have been reported in primary tumors. This difference in DNA copy number gains and losses might also contribute to the differences in gene expression between AS and AI cells. In addition, it suggests that AI cells might have a higher degree of genetic instability that contributes to their insensitivity to androgen.

Review of both the expression and DNA copy number data provides potential insights into the relatedness of the prostate cancer cell lines. For example, MDA 2a and MDA 2b, two clones originated from the same patient [27], showed highly similar gene expression and DNA copy number changes. In many studies, paired tumor samples from a single individual more closely resemble each other than they do tumors for another individual, and the similarities between the MDA cell lines likely reflect their common origin [6]. Some differences have been reported between the MDA cell lines in their growth in vivo and in vitro [27], and it is possible that the subtle differences in gene expression between them underlie these differences. PC-3 and PPC-1 that share similar karyotypes and are thought to be derived from a common source [28–30]. The striking similarities between their gene expression profiles and DNA copy number alterations substantiate this hypothesis, although some differences can be found between them. These differences might reflect clonal drift of the cell lines after years of independent growth in vitro.

Comparison of the gene expression patterns of the prostate cancer cell lines to those of surgically-resected tumors provides some insights into how well the cell lines model the disease in vivo. The gene expression patterns of the cell lines differed significantly from those of solid tumors, which may be explained in part by the fact that all of the tumors included in this study were hormone naïve, while all cell lines were derived from hormone refractory tumors. The differences observed in gene expression between cell lines and tumors may also be due to their high rates of proliferation, the absence of stromal cells, and their growth

under *in vitro* conditions. Our findings suggest caution should be used when using cell lines to model prostate carcinogenesis or progression *in vivo*. However, careful mining of the dataset revealed that some expression pathways are preserved in the cell lines that mimic those seen in different molecular subtypes of prostate cancers. Our results provide a valuable resource for experimental design and result interpretation of *in vitro* studies aimed at understanding functions of candidate genes in prostate cancer cells.

CONCLUSION

We have systematically characterized gene expression variations and DNA copy number changes in AS and independent prostate cells. Hierarchical clustering analysis separated them by their androgen sensitivity, although the genes differentially expressed between AS and AI cells are involved in a variety of biological processes such as androgen signaling and cell adhesion. Prostate cell lines tested in this study showed limited similarities in gene expression to surgically-resected prostate tumors, although they might be appropriate model systems for mechanistic studies of selected genes or pathways. The global gene expression and DNA copy number datasets in the prostate cancer cell lines could serve as a resource for prostate cancer research. Searchable versions of the datasets and the raw data are available at a companion website ([www.stanford.edu/~hongjuan/prostate cell line](http://www.stanford.edu/~hongjuan/prostate_cell_line)).

ACKNOWLEDGMENTS

Hongjuan Zhao is supported by a Postdoctoral Traineeship Award from the United States Army MPMC Prostate Cancer Research Program (Award Number W81XWH-04-1-0080).

REFERENCES

- Parkin DM, Bray FI, Devesa SS. Cancer burden in the year 2000. The global picture. *Eur J Cancer* 2001;37(Suppl 8):S4–S66.
- Jemal A, Murray T, Samuels A, Ghafoor A, Ward E, Thun MJ. Cancer statistics, 2003. *CA Cancer J Clin* 2003;53(1):5–26.
- Russell PJ, Kingsley EA. Human prostate cancer cell lines. *Methods Mol Med* 2003;81:21–39.
- Bonaccorsi L, Carloni V, Muratori M, Salvadori A, Giannini A, Carini M, Serio M, Forti G, Baldi E. Androgen receptor expression in prostate carcinoma cells suppresses alpha6beta4 integrin-mediated invasive phenotype. *Endocrinology* 2000;141(9):3172–3182.
- Bonaccorsi L, Muratori M, Carloni V, Zecchi S, Formigli L, Forti G, Baldi E. Androgen receptor and prostate cancer invasion. *Int J Androl* 2003;26(1):21–25.
- Perou CM, Sorlie T, Eisen MB, van de Rijn M, Jeffrey SS, Rees CA, Pollack JR, Ross DT, Johnsen H, Akslen LA, Fluge O, Pergamenschikov A, Williams C, Zhu SX, Lonning PE, Borresen-Dale AL, Brown PO, Botstein D. Molecular portraits of human breast tumours. *Nature* 2000;406(6797):747–752.
- Zhao H, Whitfield ML, Xu T, Botstein D, Brooks JD. Diverse effects of methylseleninic acid on the transcriptional program of human prostate cancer cells. *Mol Biol Cell* 2004;15(2):506–519.
- Pollack JR, Perou CM, Alizadeh AA, Eisen MB, Pergamenschikov A, Williams CF, Jeffrey SS, Botstein D, Brown PO. Genome-wide analysis of DNA copy-number changes using cDNA microarrays. *Nat Genet* 1999;23(1):41–46.
- Sherlock G, Hernandez-Boussard T, Kasarskis A, Binkley G, Matese JC, Dwight SS, Kaloper M, Weng S, Jin H, Ball CA, Eisen MB, Spellman PT, Brown PO, Botstein D, Cherry JM. The Stanford Microarray Database. *Nucleic Acids Res* 2001;29(1):152–155.
- Wang P, Kim Y, Pollack JR, Tibshirani R. Cluster along chromosomes (CLAC) a method for array CGH analysis. *Biostatistics* 2004.
- Eisen MB, Spellman PT, Brown PO, Botstein D. Cluster analysis and display of genome-wide expression patterns. *Proc Natl Acad Sci USA* 1998;95(25):14863–14868.
- Tusher VG, Tibshirani R, Chu G. Significance analysis of microarrays applied to the ionizing radiation response. *Proc Natl Acad Sci USA* 2001;98(9):5116–5121.
- Qi H, Fillion C, Labrie Y, Grenier J, Fournier A, Berger L, El-Afy M, Labrie C. AlbZIP, a novel bZIP gene located on chromosome 1q21.3 that is highly expressed in prostate tumors and of which the expression is up-regulated by androgens in LNCaP human prostate cancer cells. *Cancer Res* 2002;62(3):721–733.
- Sun Z, Pan J, Balk SP. Androgen receptor-associated protein complex binds upstream of the androgen-responsive elements in the promoters of human prostate-specific antigen and kallikrein 2 genes. *Nucleic Acids Res* 1997;25(16):3318–3325.
- Korkmaz KS, Korkmaz CG, Ragnhildstveit E, Kizildag S, Pretlow TG, Saatcioglu F. Full-length cDNA sequence and genomic organization of human NKX3A—Alternative forms and regulation by both androgens and estrogens. *Gene* 2000;260(1–2):25–36.
- Lin B, Ferguson C, White JT, Wang S, Vessella R, True LD, Hood L, Nelson PS. Prostate-localized and androgen-regulated expression of the membrane-bound serine protease TMPRSS2. *Cancer Res* 1999;59(17):4180–4184.
- DePrimo SE, Diehn M, Nelson JB, Reiter RE, Matese J, Fero M, Tibshirani R, Brown PO, Brooks JD. Transcriptional programs activated by exposure of human prostate cancer cells to androgen. *Genome Biol* 2002;3(7):Research0032.
- Ashburner M, Ball CA, Blake JA, Botstein D, Butler H, Cherry JM, Davis AP, Dolinski K, Dwight SS, Eppig JT, Harris MA, Hill DP, Issel-Tarver L, Kasarskis A, Lewis S, Matese JC, Richardson JE, Ringwald M, Rubin GM, Sherlock G. Gene ontology: Tool for the unification of biology. The Gene Ontology Consortium. *Nat Genet* 2000;25(1):25–29.
- Lapointe J, Li C, Higgins JP, van de Rijn M, Bair E, Montgomery K, Ferrari M, Egevad L, Rayford W, Bergerheim U, Ekman P, DeMarzo AM, Tibshirani R, Botstein D, Brown PO, Brooks JD, Pollack JR. Gene expression profiling identifies clinically relevant subtypes of prostate cancer. *Proc Natl Acad Sci USA* 2004;101(3):811–816.
- Whitfield ML, Sherlock G, Saldanha AJ, Murray JI, Ball CA, Alexander KE, Matese JC, Perou CM, Hurt MM, Brown PO, Botstein D. Identification of genes periodically expressed in the human cell cycle and their expression in tumors. *Mol Biol Cell* 2002;13(6):1977–2000.
- Culig Z. Role of the androgen receptor axis in prostate cancer. *Urology* 2003;62(5 Suppl 1):21–26.

22. Holzbeierlein J, Lal P, LaTulippe E, Smith A, Satagopan J, Zhang L, Ryan C, Smith S, Scher H, Scardino P, Reuter V, Gerald WL. Gene expression analysis of human prostate carcinoma during hormonal therapy identifies androgen-responsive genes and mechanisms of therapy resistance. *Am J Pathol* 2004; 164(1):217–227.
23. Zhang L, Johnson M, Le KH, Sato M, Ilagan R, Iyer M, Gambhir SS, Wu L, Carey M. Interrogating androgen receptor function in recurrent prostate cancer. *Cancer Res* 2003;63(15): 4552–4560.
24. Gregory CW, Johnson RT Jr., Mohler JL, French FS, Wilson EM. Androgen receptor stabilization in recurrent prostate cancer is associated with hypersensitivity to low androgen. *Cancer Res* 2001;61(7):2892–2898.
25. Amler LC, Agus DB, LeDuc C, Sapinoso ML, Fox WD, Kern S, Lee D, Wang V, Leysens M, Higgins B, Martin J, Gerald W, Dracopoli N, Cordon-Cardo C, Scher HI, Hampton GM. Dysregulated expression of androgen-responsive and nonresponsive genes in the androgen-independent prostate cancer xenograft model CWR22-R1. *Cancer Res* 2000;60(21):6134–6141.
26. Pollack JR, Sorlie T, Perou CM, Rees CA, Jeffrey SS, Lonning PE, Tibshirani R, Botstein D, Borresen-Dale AL, Brown PO. Microarray analysis reveals a major direct role of DNA copy number alteration in the transcriptional program of human breast tumors. *Proc Natl Acad Sci USA* 2002;99(20):12963–12968.
27. Navone NM, Olive M, Ozen M, Davis R, Troncoso P, Tu SM, Johnston D, Pollack A, Pathak S, von Eschenbach AC, Logothetis CJ. Establishment of two human prostate cancer cell lines derived from a single bone metastasis. *Clin Cancer Res* 1997; 3(12 Pt 1):2493–2500.
28. Chen TR. Chromosome identity of human prostate cancer cell lines, PC-3 and PPC-1. *Cytogenet Cell Genet* 1993;62(2–3):183–184.
29. van Bokhoven A, Varella-Garcia M, Korch C, Hessels D, Miller GJ. Widely used prostate carcinoma cell lines share common origins. *Prostate* 2001;47(1):36–51.
30. Varella-Garcia M, Boomer T, Miller GJ. Karyotypic similarity identified by multiplex-FISH relates four prostate adenocarcinoma cell lines: PC-3, PPC-1, ALVA-31, and ALVA-41. *Genes Chromosomes Cancer* 2001;31(4):303–315.